6 Transperineal Ultrasonography: Methodology and Normal Pelvic Floor Anatomy

Hans Peter Dietz

Learning Objectives

- To appreciate the basic methodology of translabial/perineal ultrasound using 2D and 3D/4D systems.
- To understand the basic functional anatomy of the female pelvic floor.
- To recognize normal anatomical structures both in the midsagittal and the axial plane.
- To identify the levator ani and the anal sphincter in tomographic imaging.

6.1 Introduction

Ultrasound is the primary imaging method in gynecology and commonly used in urology and colorectal surgery. Hence it is not surprising that it is increasingly popular in the imaging assessment of pelvic floor anatomy. This development is long overdue, seeing that pathophysiology and etiology of many pelvic floor conditions are still poorly understood at present. The evaluation of urethral and paraurethral anatomy and pelvic organ mobility has become easier due to recent technological developments [1]. The same applies to the assessment of defecatory dysfunction [2]. The advent of 3D ultrasound now allows access to the axial plane, and 4D ultrasound enables the observation of function in the form of maneuvers such as cough, Valsalva, and pelvic floor muscle contraction [3]. Tomographic techniques are increasingly used for the assessment of birth trauma to levator ani [4] and anal sphincter muscles [5] which will become a key performance indicator of obstetric services and change maternity services delivery worldwide [6].

Other techniques such as endovaginal and endo-anal ultrasound have been used in the investigation of pelvic floor disorders, but this chapter will exclusively cover translabial or transperineal ultrasound which, for the sake of simplicity, the author calls "pelvic floor ultrasound." This modality is unique in that it allows a comprehensive assessment of pelvic floor structures in one single, noninvasive investigation of at most 10 min duration. It can replace video cystourethrography, magnetic resonance imaging, defecation proctography, and endo-anal ultrasound in women suffering from symptoms of lower urinary tract dysfunction, prolapse, obstructed defecation, and fecal incontinence, using systems almost universally available. Chapter 48 will cover pathological findings, while this chapter deals with normal anatomy.

The definition of "normal" is fundamental to the practice of medicine. Without "normal" there is no "abnormal" and no basis for therapeutic intervention. This is particularly true in a newly developed diagnostic field such as pelvic floor ultrasound. Overdiagnosis, that is, the risk of misinterpreting findings as abnormal that are in fact within the normal range, is always a danger. Hence I will try to define "normal," both in terms of static anatomy and in terms of "dynamic anatomy," i.e., function, as far as it applies to urogynecological conditions.

6.2 Basic Technique

The basic requirements for pelvic floor imaging include a B-mode capable two-dimensional (2D) ultrasound system with cine-loop function, a 3.5–6 MHz curved array transducer, and a videoprinter. However, to allow for the full scope of diagnostic capabilities, 3D/4D imaging is indispensable. For over 20 years, Voluson-type systems have been the market leaders in the field of 3D/4D ultrasound. Consequently most of the literature on 3D pelvic floor ultrasound is based on the utilization of such systems, even if most manufacturers now offer equipment that can be employed usefully. Any 4D capable ultrasound system with abdominal 4D transducers in an obstetric imaging unit

H. P. Dietz (✉)
Sydney Medical School Nepean, University of Sydney, Sydney, NSW, Australia
e-mail: hpdietz2@bigpond.com

G. A. Santoro et al. (eds.), *Pelvic Floor Disorders*, https://doi.org/10.1007/978-3-030-40862-6_6

should be suitable for pelvic floor ultrasound, provided the aperture angle is 70° or better and provided the acquisition angle can be set to at least 70°. For severe prolapse and hiatal ballooning, aperture and acquisition angles of 80–90° can become necessary.

The examination is performed in dorsal lithotomy with the hips flexed and slightly abducted or alternatively in the standing position. Asking the patient to place her heels close to the buttocks will result in an improved pelvic tilt. A full bladder or bowel may prevent full development of pelvic organ prolapse [7]. Therefore, imaging is best performed after bladder emptying; otherwise bladder filling should be specified. Occasionally, catheterization will be necessary.

For preparation of the probe, it is covered with either a powder-free glove, condom, or thin plastic wrap for hygienic purposes, after covering the transducer surface with ultrasound gel and while avoiding air bubbles between transducer surface and glove. The probe is then placed on the perineum after parting the labia, producing a midsagittal view showing urethra and anal canal at the same time (see Fig. 6.1). Tissue hydration and scar tissue can affect visibility, but obesity is virtually never a problem. Conditions are best in pregnancy and poorest in the senium. The probe can be placed firmly without causing significant discomfort, unless there is marked atrophy or vulvitis. During a Valsalva it is essential, however, not to exert undue pressure to allow full development of pelvic organ descent. After scanning the probe is mechanically cleaned, followed by disinfection with alcoholic wipes. Sterilization as for intracavitary transducers is usually considered unnecessary.

On translabial ultrasound, pelvic floor structures are initially shown in the midsagittal plane [1]. This orientation, shown in Fig. 6.1, allows imaging of the urethra, the bladder neck and trigone, the cervix, the rectal ampulla, and the anal canal. While there is no universal consensus on image orientation, the first published translabial images had the perineum at the top and the symphysis pubis on the left [7], and this is still the most commonly used orientation. It is particularly convenient when using three-dimensional (3D)/four-dimensional (4D) systems as shown in Fig. 6.2. The top left image represents the midsagittal plane, with the bottom right showing a rendered volume of the levator hiatus.

The advent of 3D/4D imaging has given easy, noninvasive access to the axial plane allowing imaging of the caudal part of the levator ani muscle and the opening in this muscular plate, the levator hiatus (Fig. 6.2). The levator hiatus is an important part of the birth canal and the largest potential hernial portal in the human body. It is of central importance in the pathophysiology of female pelvic organ prolapse (POP), a highly prevalent condition that may require surgery at least once during the lifetime of 10–20% of the female population [8, 9].

POP is best understood as a hernia through the levator hiatus. In childbirth the hiatus is distended massively [10], and the limiting structure, the puborectalis muscle, runs a substantial risk of permanent damage, either due to irreversible overdistension or due to actual disruption in the shape of avulsion, i.e., disconnection from its insertion on the os pubis [11, 12]. Both forms of trauma seem to be risk factors for POP and POP recurrence after reconstructive surgery [13–16]. Hence, imaging of the levator hiatus and puborectalis muscle in axial plane images is becoming increasingly popular.

Most recently, the coronal plane has attracted increasing interest as it provides excellent views of the anal canal, especially the anal sphincter complex, and volume acquisition is optimally performed in the coronal plane, as shown in Fig. 6.3. The increasing prevalence of anal sphincter trauma, especially in jurisdictions with rising forceps rates such as in the UK and Australia [17], makes the development of this method particularly timely and important.

Fig. 6.1 Transducer placement on the perineum (left) with schematic representation of the resulting midsagittal field of vision. Right image adapted from [1], with permission

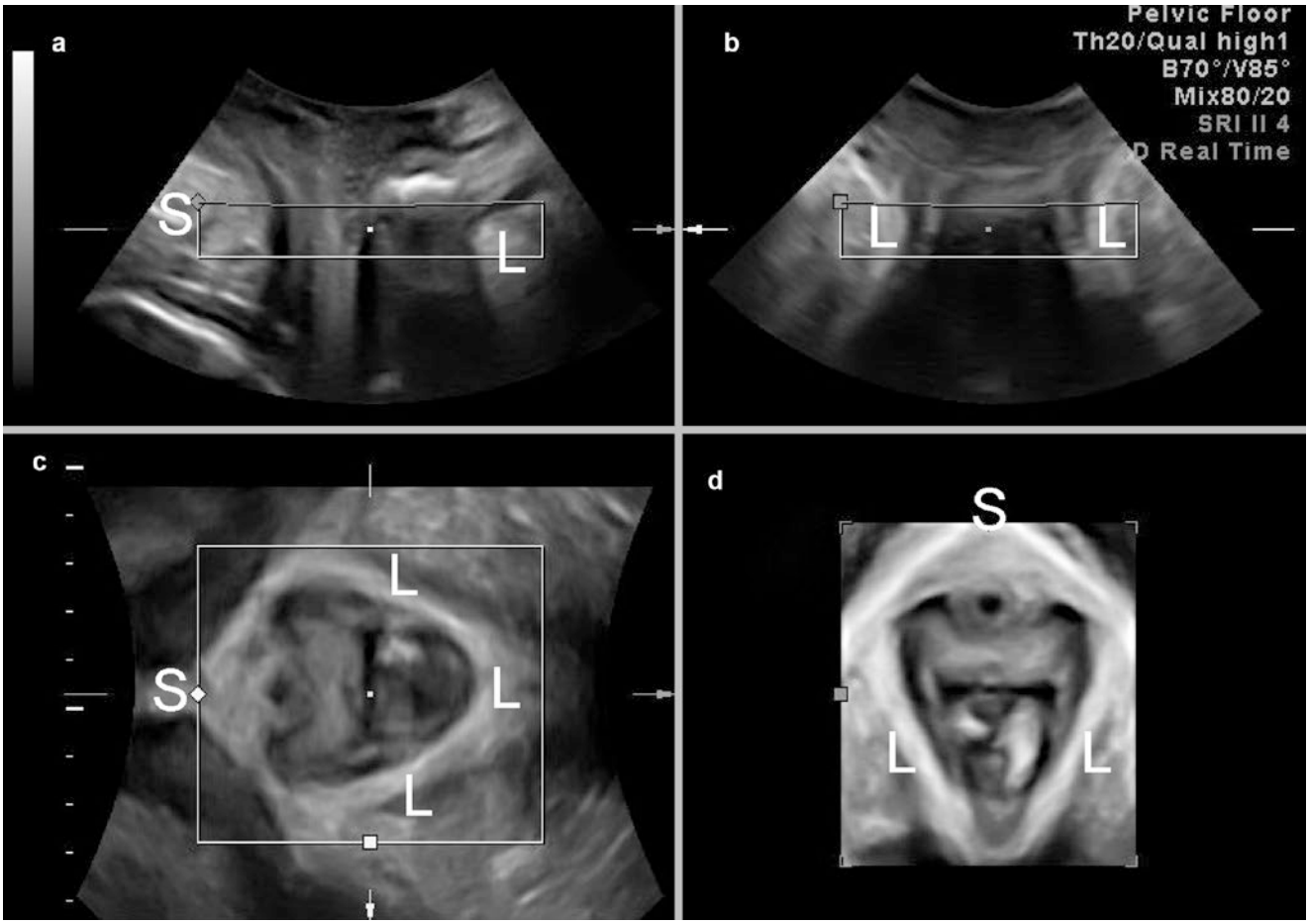

Fig. 6.2 Standard representation of female pelvic floor structures on translabial/perineal ultrasound. The midsagittal plane is shown in (**a**), the coronal in (**b**), the axial in (**c**). A rendered volume (i.e., the semitransparent representation of all pixels in the "region of interest," the box seen in **a**–**c**) in the axial plane is given in (**d**). Often, **a** and **d** are of the most interest and are combined, leaving out **b** and **c**. In **d** the patient's right-hand side is represented on the left, as if the pelvic floor was viewed from below. *L* levator ani, *S* symphysis pubis. From [74], with permission

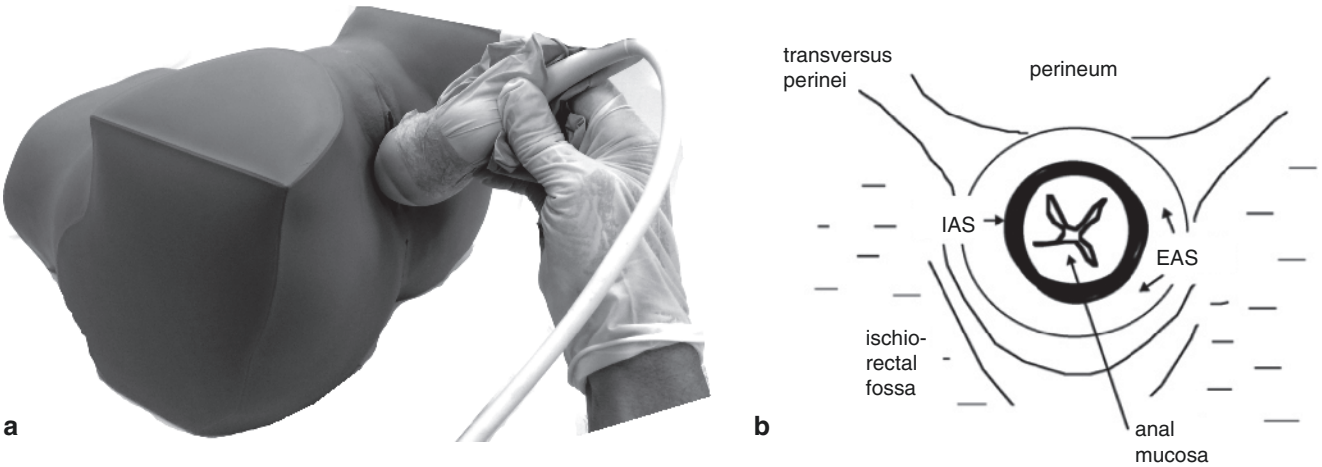

Fig. 6.3 Transducer placement for exo-anal sphincter imaging (left), and schematic illustration of imaged structures in the resulting coronal or transverse plane (right). *EAS* external anal sphincter, *IAS* internal anal sphincter. From [32], with permission

Live anatomy of pelvic floor structures as observed on real-time imaging commonly bears only limited resemblance to textbook illustrations. The "urogenital diaphragm" is a figment of the imagination to those performing translabial ultrasound. The levator plate appears very different from textbook illustrations derived from cadaver dissection, and the anal canal is longer and slimmer in reality than in drawings derived from endo-anal ultrasound which necessarily dilates and shortens this structure. Common forms of prolapse such as cystocele and rectocele appear rather different from textbook illustrations when imaged live.

Given that cadaver dissection and illustrations derived from dissection are frequently misleading, it seems appropriate to use this chapter to describe the normal anatomy of the pelvic floor as seen on 3D/4D pelvic floor ultrasound.

6.3 The Anterior Compartment: Urethra and Bladder Base

6.3.1 The Urethra

The female urethra is a muscular tube of about 3–3.5 cm in length, made up principally of a smooth muscle layer (the longitudinal smooth muscle of the urethra) and the striated urethral sphincter, which surrounds the smooth muscle like an elongated, spindle-shaped torus. At rest the smooth muscle is hypoechoic, and the striated muscle hyperechogenic, as seen in Fig. 6.4. The rhabdosphincter is better appreciated in the axial plane where it is apparent as a hyperechoic ring shape; in the midsagittal plane, it is harder to see due to the echogenicity of retropubic fibrofatty tissue. Echogenicity of smooth and striated urethral muscle changes with the angle of the incident beam, i.e., the angle between urethra and transducer. On Valsalva the urethra frequently rotates around the symphysis pubis, changing the angle between urethral structures and the incident beam; and the hypoechogenic stripe of urethral smooth muscle seems to disappear (Fig. 6.5). If the urethra rotates more than 90°, it may "reappear" once the smooth muscle of the proximal urethra is again more parallel with the incident beam, which often occurs in severe cystocele.

6.3.2 Paraurethral Tissues

This muscular tube is anchored to the pelvic sidewall or, rather, the os pubis. This anchoring is highly variable, with anywhere between 1 and 7 distinct structures [18] made up of varying amounts of connective tissue and smooth muscle fibers. These structures are generally termed the "pubourethral ligaments" and can be visualized in the coronal plane (Fig. 6.6). The functional effect of those ligaments is commonly observed in the form of urethral kinking and a demonstration of the concept of pressure, or rather, force transmission at times of increased intra-abdominal pressure. Tethering of the urethra to the os pubis is clearly important for urinary stress continence [19]. Figure 6.7 shows marked urethral kinking, which is common in anterior compartment prolapse.

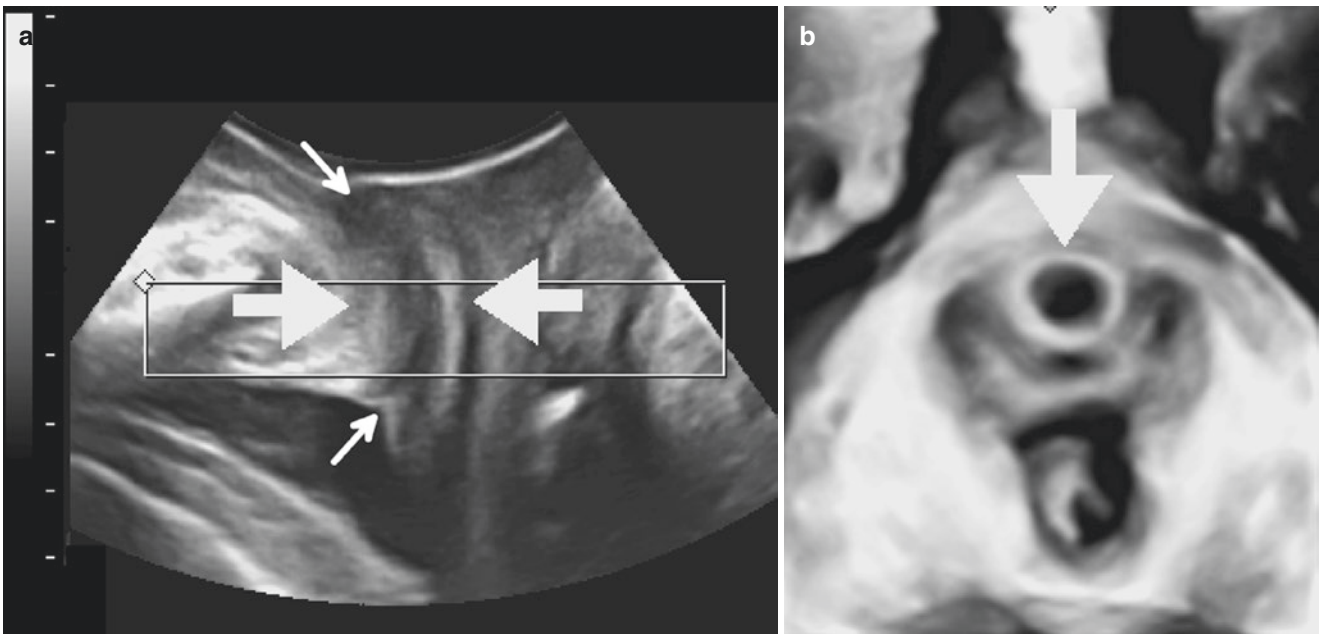

Fig. 6.4 The urethra as seen on translabial 4D ultrasound. The midsagittal plane is on the left (**a**). Small arrows show the external meatus at the top, and the internal urethral meatus at the bottom. Large arrows indicate the urethral rhabdosphincter which appears as two hyperechoic stripes on the left and as a hyperechoic ring shape on the right (**b**)

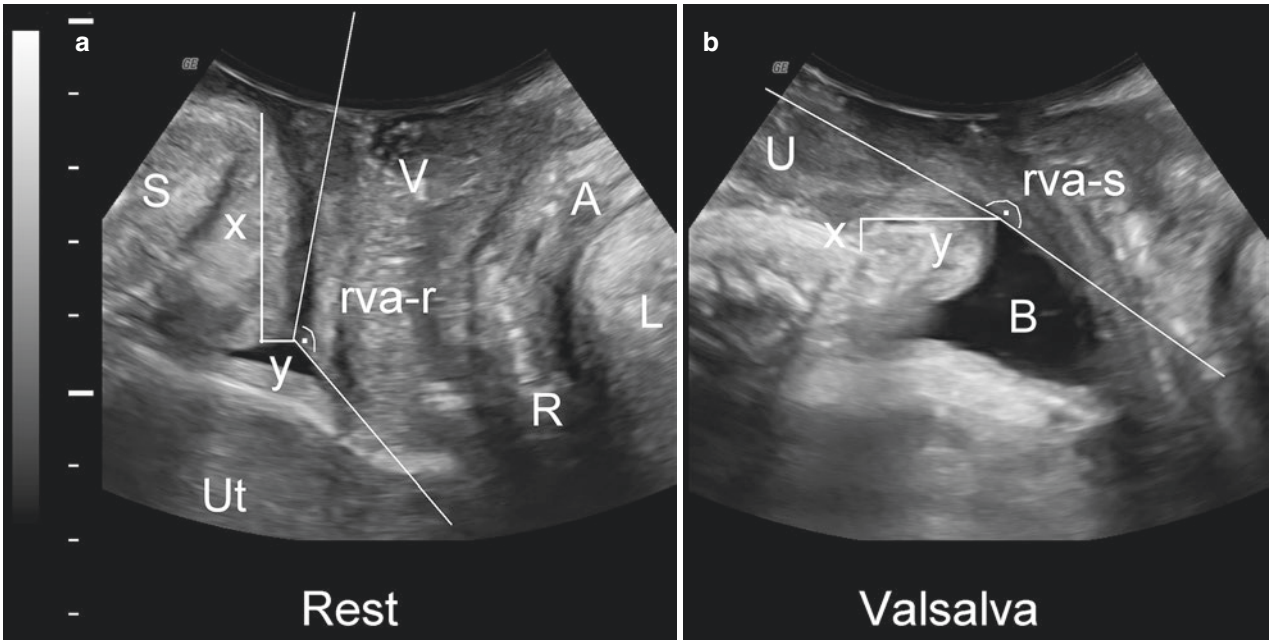

Fig. 6.5 Determination of bladder neck descent and retrovesical angle: Ultrasound images show the midsagittal plane at rest (**a**) and on Valsalva (**b**). *A* anal canal, *B* bladder, *L* levator ani, *R* rectal ampulla, *S* symphysis pubis, *U* urethra, *Ut* uterus, *V* vagina. The images demonstrate the measurement of distances between interior symphyseal margin and bladder neck (vertical, *x*; horizontal, *y*) and the retrovesical angle at rest (rva-r) and on Valsalva (rva-s). From [53], with permission

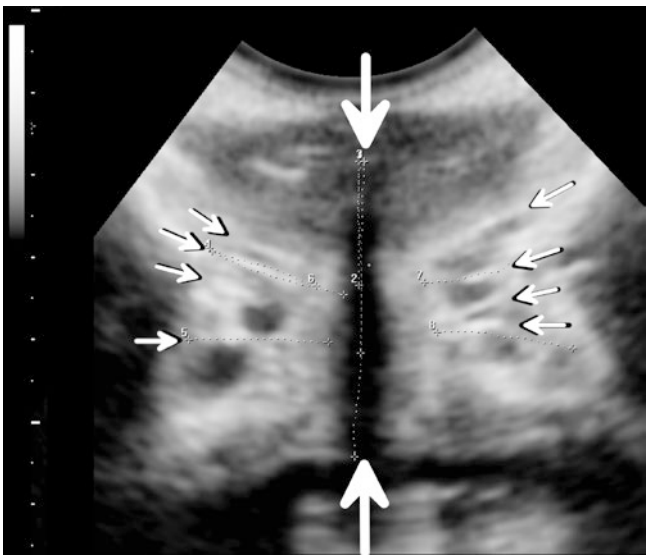

Fig. 6.6 Coronal plane imaging showing the length of the urethra (large arrow to large arrow) and multiple linear structures (small arrows) investing the urethral rhabdosphincter surrounding the hypoechogenic longitudinal smooth muscle/vascular plexus/mucosa of the urethra

6.3.3 The Bladder Neck and Trigone

The bladder neck, i.e., the urethrovesical junction or internal meatus of the urethra, is visible as a "notch" or a slight dimple on translabial imaging. Approximately 1–2 cm dorsal to this dimple one will find the inter-ureteric ridge, which can be followed laterally to reach the ureteric orifices. The "trigone" or bladder base is formed by thickened smooth muscle between the internal meatus and the two ureteric orifices. If desired, color Doppler can be used to demonstrate ureteric patency. The detrusor muscle (Fig. 6.8) is usually thinner than the trigone itself. Its thickness is associated with symptoms of the overactive bladder and with urodynamic detrusor overactivity. Under 50 ml bladder filling, 5 mm is regarded as the limit of normal [20–22], but DWT has poor test characteristics for urge urinary incontinence and detrusor overactivity [22, 23].

6.4 The Fornices

The anterior vaginal fornices have been of interest as they are clinically easily accessible for the assessment of paravaginal or bladder fascia, although clinical examination seems of limited validity and reproducibility [24, 25]. Often, an abnormal fornix means not just fascial damage, but rather much more severe trauma in the shape of levator avulsion. However, there may be a subset of women in whom the levator is intact but the paravaginal fascia is detached from the arcus tendineus fasciae pelvis, and this may be evident as a loss of forniceal definition [26]. On axial plane imaging, the fornices are plainly visible, especially in their lower reaches (Fig. 6.9). Tomographic imaging on Valsalva seems to be useful in assessing the fornices more cranially (Fig. 6.10).

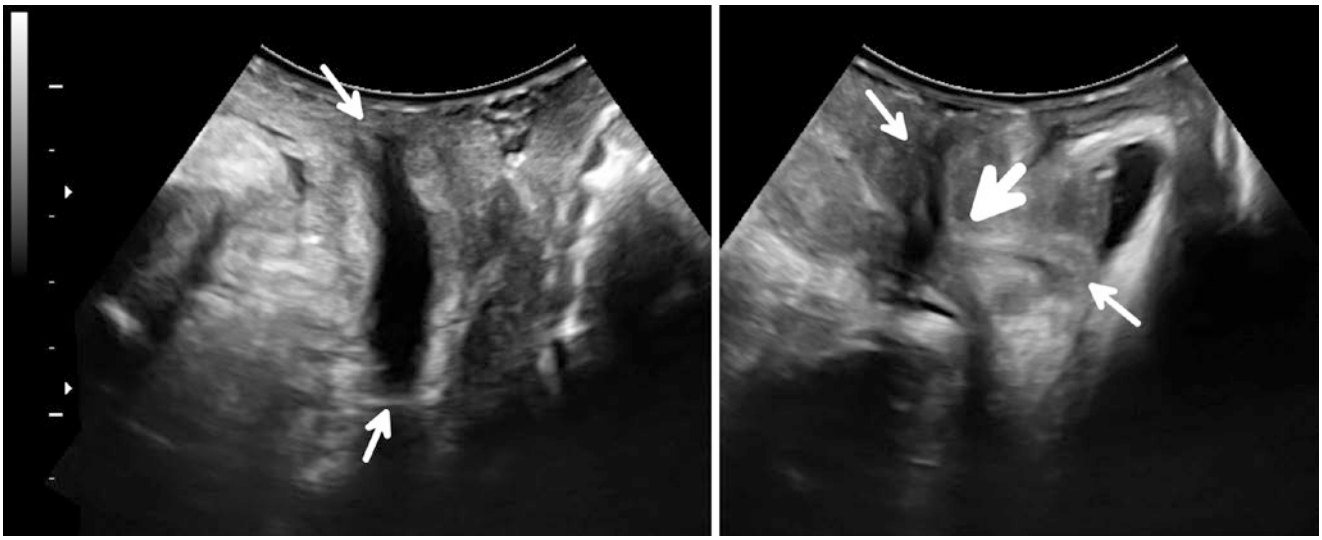

Fig. 6.7 Midsagittal imaging at rest (left) and on Valsalva (right) in patient with grade II cystocele. There is marked urethral kinking at mid-urethral level, i.e., at the location of urethral tethering to the pelvic sidewall. The small arrows indicate external and internal urethral meatus, and the large arrow the location of urethral kinking. The variability of urethral echogenicity relative to the angle between urethra and incident beam is also clearly apparent

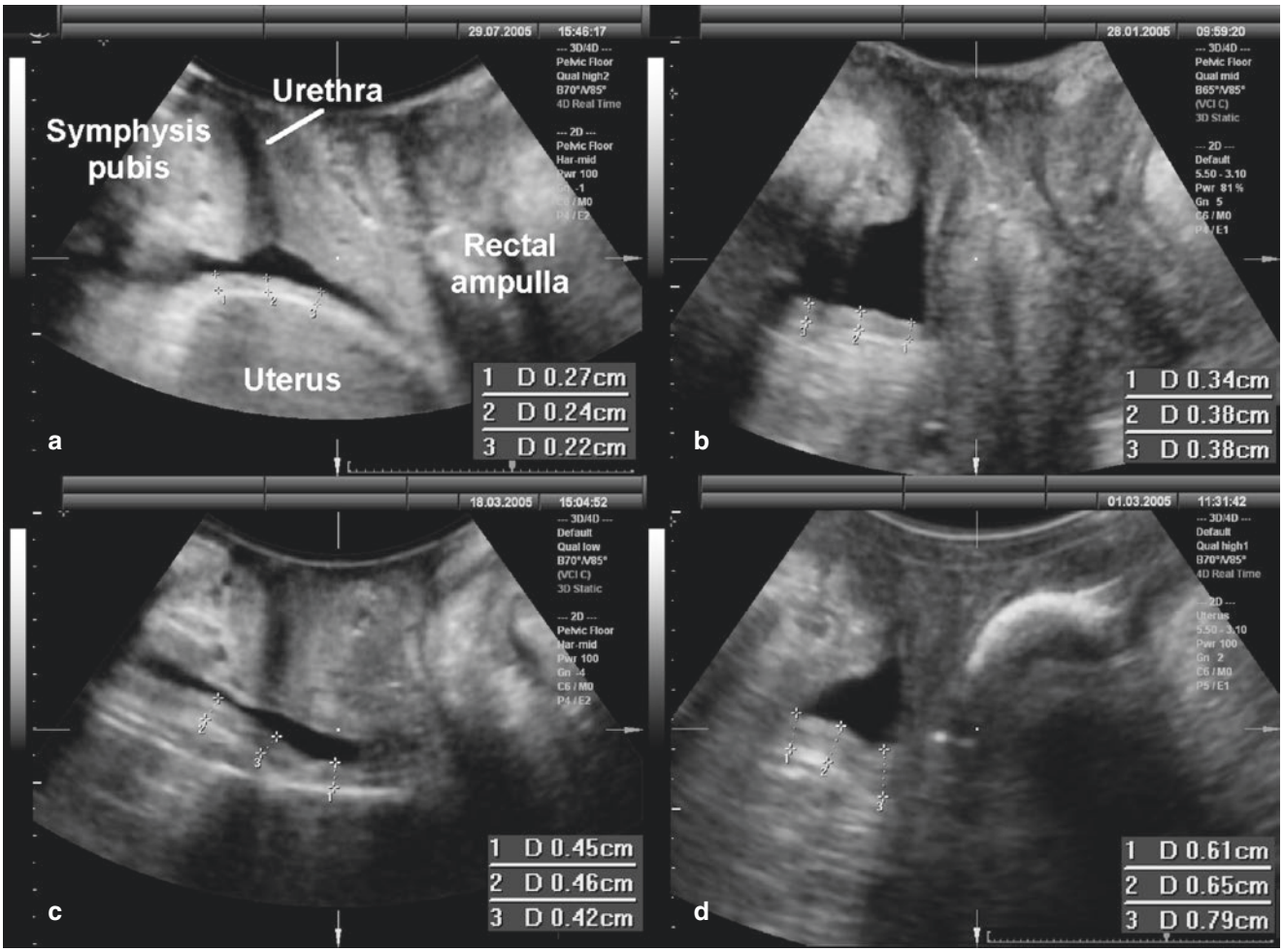

Fig. 6.8 Measurement of bladder wall thickness at the dome in four women with non-neuropathic bladder dysfunction. In all cases shown in images (**a**–**d**) residual urine is well below 50 ml. The limit of normality is usually taken to be 5 mm. From [74], with permission

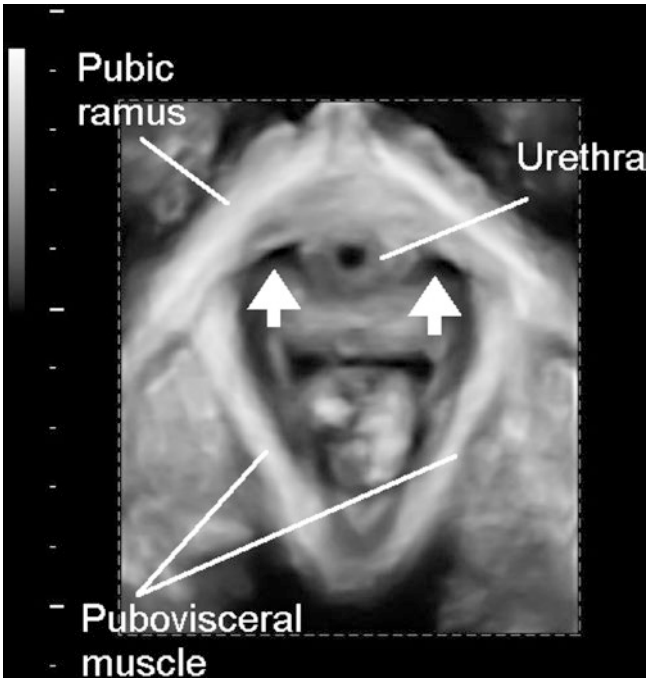

Fig. 6.9 The appearance of puborectalis muscle and lateral vaginal fornices in a rendered volume in the axial plane. The two arrows indicate the fornices. From [75], with permission

6.5 The Central Compartment: Uterus and Vault

The anteverted uterus is visible above the bladder roof, with the endometrial stripe identifiable as a near-horizontal line that can be followed to the cervical canal (Fig. 6.11). In retroversion the cervix may be harder to identify, and small bowel covers the bladder roof. The cervix may be shadowed by rectal ampulla, if it is filled with stool and/or gas. A small, atrophic uterus is sometimes very difficult to locate, especially if high. As the myometrium is iso-echoic and very similar in echogenicity to the vaginal walls, identifying the uterus can be a challenge for the beginner, but often nabothian follicles help in identifying the cervix. In general, moving images are easier to interpret, and this is especially true for the uterus. In older women and in an axial uterus, the myometrium can cause acoustic shadowing due to scattering of ultrasonic energy, and this may also be the case with fibroids, especially if calcified. After hysterectomy, the space usually occupied by the uterus is filled by peristalsing small bowel. The vault itself may at times be easy to locate (Fig. 6.12); at other times it will be hidden by a full rectum unless the vault descends beyond the hymen.

6.6 The Posterior Compartment

6.6.1 Normal Anatomy in the Midsagittal Plane

The standard midsagittal orientation is defined by both anal canal and urethra being visible in one plane which shows the rectal ampulla, often stool-filled, the anorectal angle, and the anal canal, a tubular structure about 4.5 cm in length. The anorectal junction is easy to identify, either due to the hyperechoic nature of stool or bowel gas in the rectal ampulla or due to the iso-echoic anal mucosal folds occupying the space between the two hypoechogenic linear strips of the internal anal sphincter (IAS).

6.6.2 The Perineal Body/Transversus Perinei

Ventrocaudal to the anal canal, one can locate the triangular iso-echoic structure of the perineal body, which is highly variable in dimensions even in nulliparous women [27]. It is bounded by the vagina ventrally (outlined more clearly after a vaginal examination due to bubbles caught in the vaginal rugae) and the external anal sphincter dorsally. Its most distinct structure, the transversus perinei muscle, is also very variable but often identified in the coronal plane (Fig. 6.13) where, on imaging of the anal sphincter, it often appears as a linear or wing-like structure, the fibers of which may contribute to the more cranial aspects of the external anal sphincter (EAS), occasionally causing a hose clamp-like appearance.

6.6.3 The Rectovaginal Septum

The rectovaginal septum (RVS) is the cranial continuation and condensation of the fibromuscular perineal body and sometimes visible on perineal imaging; see Fig. 6.14. It is a fascia that prevents herniation of the rectal ampulla into the lower vagina, given that there is a substantial pressure differential between the former (intra-abdominal pressure) and the latter (atmospheric pressure) [28]. Dynamic testing with a Valsalva maneuver is required to detect RVS defects as static appearances do not seem to be predictive of function [29]. Such defects are very common, even in nulliparae [30], and represent the only form of prolapse that is clearly associated with obesity [31].

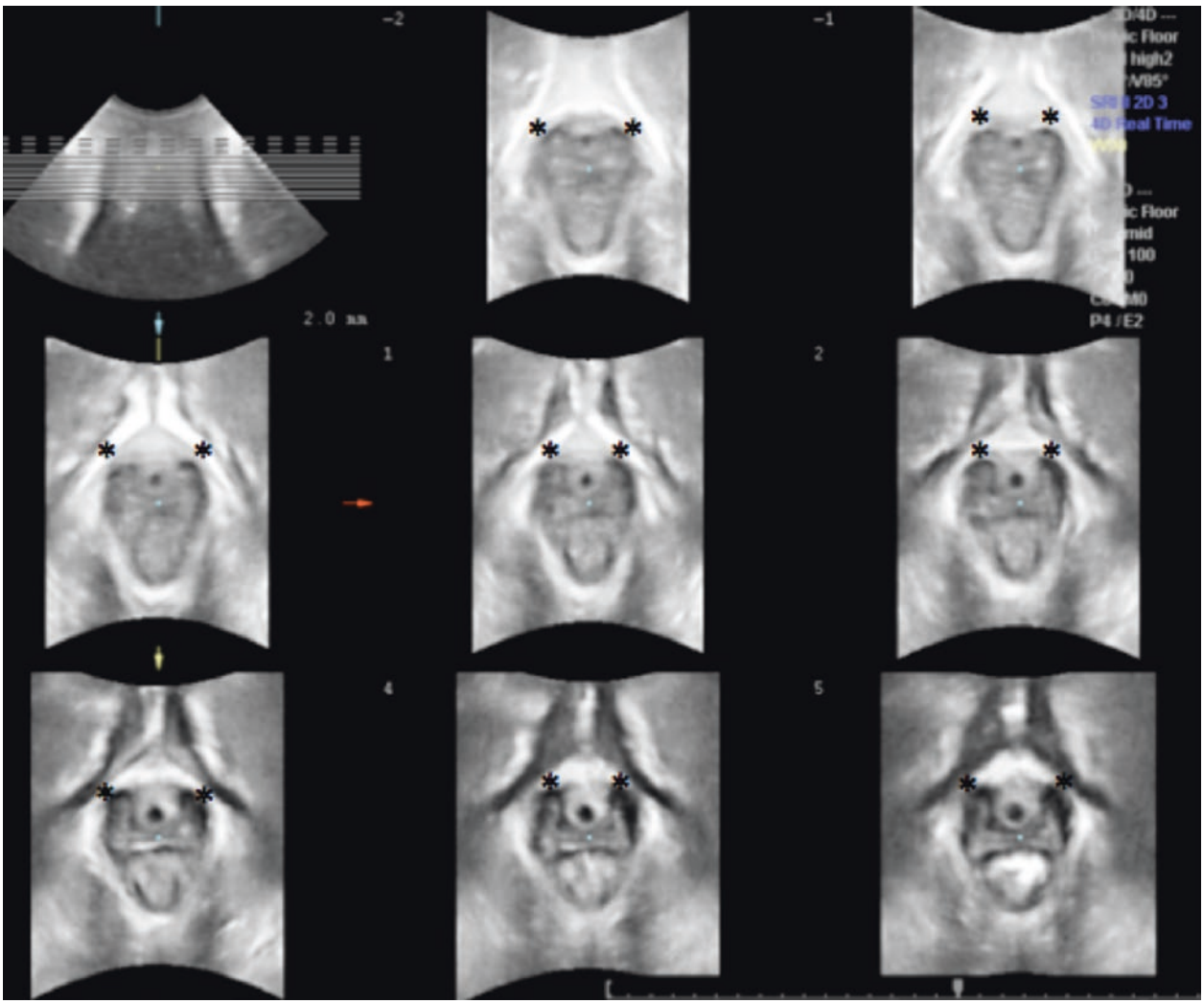

Fig. 6.10 Fornices are assessed by tomographic ultrasound, with eight slices obtained from the plane of minimal hiatal dimensions to 12.5 mm above this plane. In the figure, the fornices are all intact (i.e., showing a triangular appearance, with the apex aiming toward the os pubis) and indicated with (∗). From [26], with permission

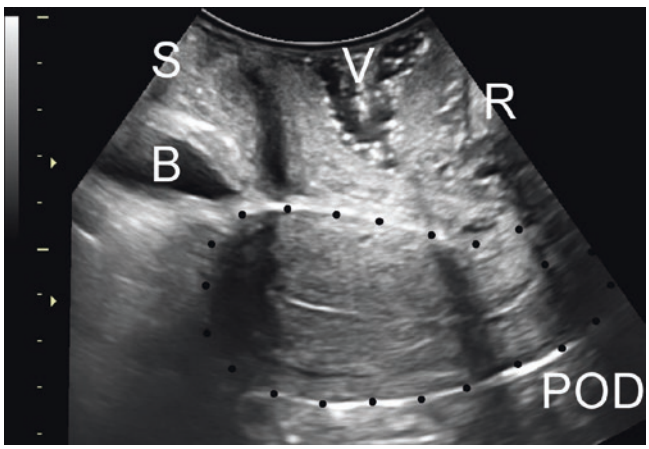

Fig. 6.11 Anteverted uterus as seen in the midsagittal plane, with the corpus resting on the roof of the empty bladder. The cervix is just visible cranial to the rectal ampulla which often obscures a normally situated cervix. *B* bladder, *POD* pouch of Douglas, *R* rectal ampulla, *S* symphysis pubis, *V* vagina. The uterus is outlined by dots; both cervix and endometrial echo are clearly visible

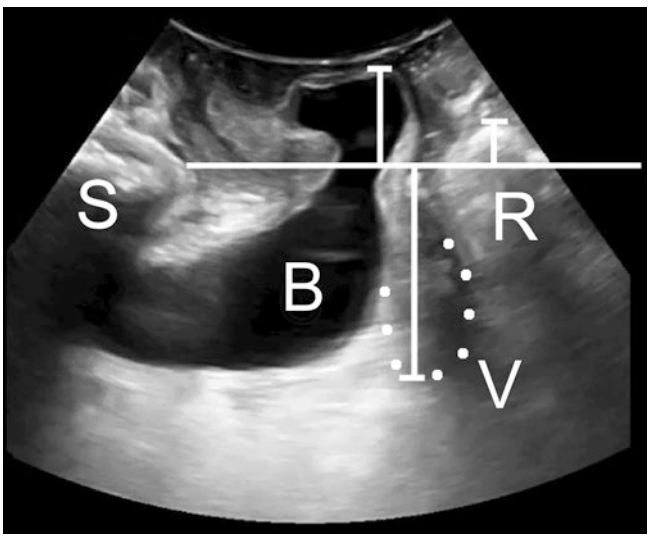

Fig. 6.12 Appearance of a normal, well-supported vaginal vault in patient with stage 2 cystocele. The position of bladder (B), vault (V), and rectal ampulla (R) are measured against the inferoposterior margin of the symphysis pubis (S)

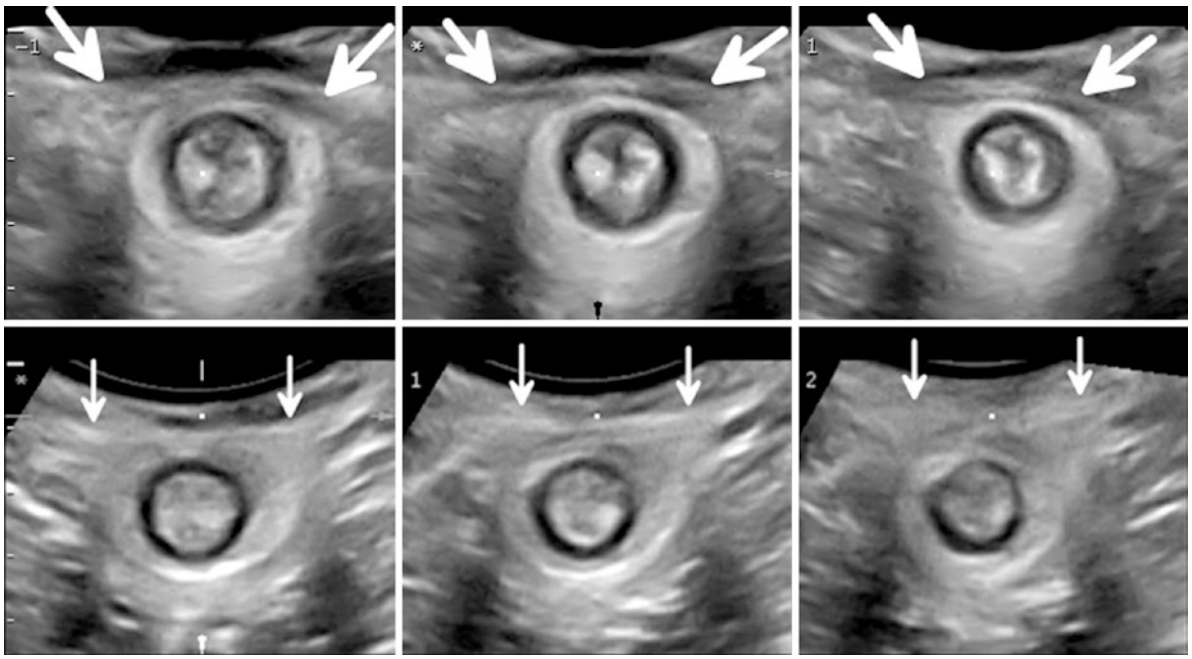

Fig. 6.13 The echogenicity and appearance of the perineum vary greatly even in vaginally nulliparous women. However, in the latter it is often possible to identify a hyperechoic transverse structure superficial to the external anal sphincter (EAS); see those tomographic transverse slices of the perineum. Sometimes fibers seem to be completely separate from the EAS (top row; fat oblique arrows); at other times some fibers clearly merge with the EAS (bottom row; thin vertical arrows)

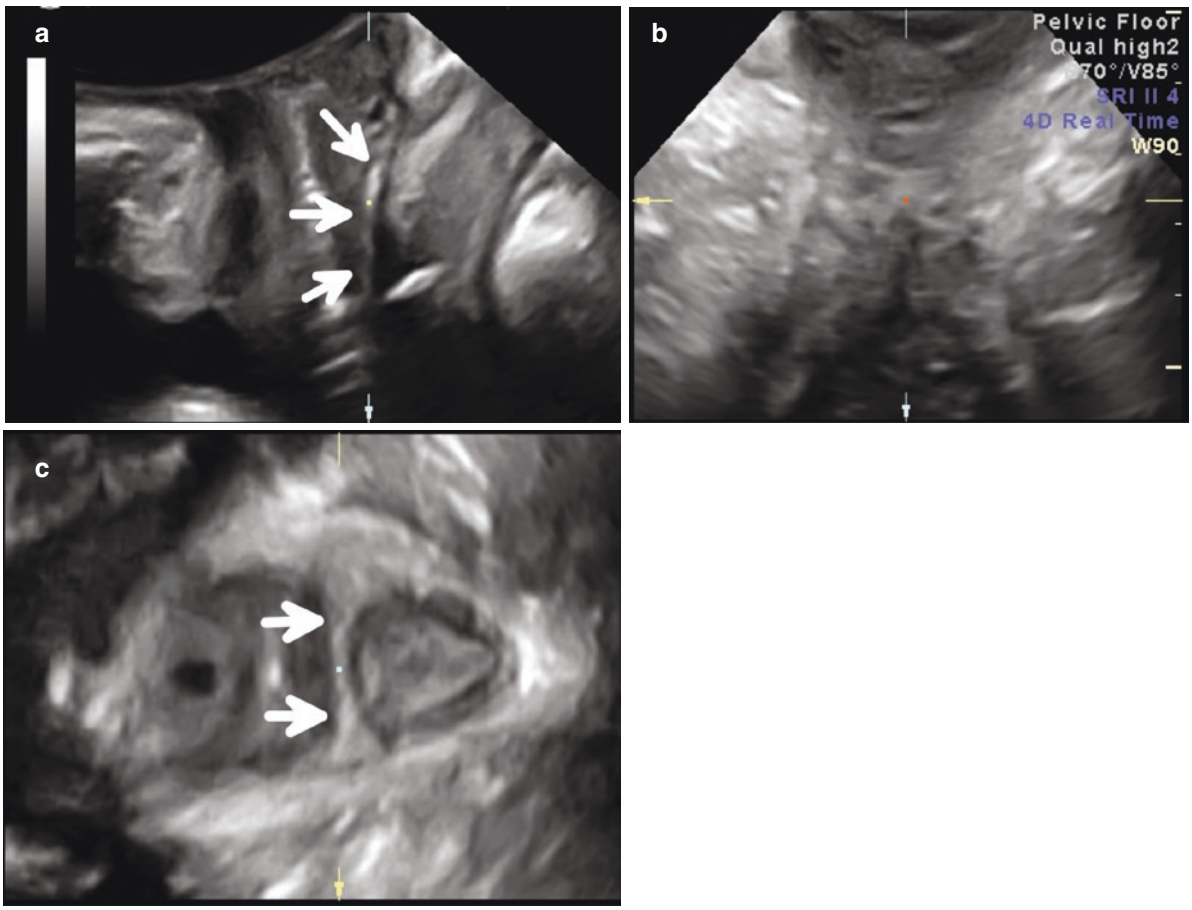

Fig. 6.14 Appearance of a presumably intact rectovaginal septum on 3D pelvic floor imaging in orthogonal planes (**a**–**c**). Arrow indicates the location of the septum which appears as a linear hyperechogenic structure in the midsagittal (**a**) and axial (**c**) plane

6.6.4 The Anal Canal on Tomographic Imaging

The anal canal and rectal ampulla are conveniently imaged in the midsagittal plane, but this is not the case for the anal sphincters. Traditionally, sphincter imaging is undertaken by endo-anal probes which provide a coronal plane view of the sphincters, visualizing them as donut- or target-shaped structures. On pelvic floor ultrasound, this requires rotation of the transducer to the coronal plane (see Fig. 6.3). Volume acquisition at 60–70° aperture and acquisition angle, with harmonics set to "high" and focal zones adjusted to sit at the depth of the area of interest, provides optimal imaging. A pelvic floor muscle contraction and adjustment of transducer pressure may also help to optimize resolutions. The distance between external anal sphincter and transducer surface is highly variable, not the least due to the state of the perineum, but is easily adjusted by holding the transducer at a rather steep angle (more vertical than horizontal) and by varying the position of the transducer relative to the fourchette and anus.

A view of the three sectional planes allows centering of the sphincter in the volume (Fig. 6.15). The anal canal should be horizontal in the B (midsagittal) plane and vertical in the C (transverse) plane, an orientation that helps identify the cranial extent of the EAS (Fig. 6.16) by locating the fascial plane between EAS and levator ani. The EAS is then imaged in tomographic slices, from above the EAS cranially to the subcutaneous EAS below the termination of the IAS caudally (Fig. 6.17) [32]. Depending on EAS length, which can vary from 8 to 35 mm in healthy individuals [33], the interslice interval may have to be set to anywhere from 1.5 to 5 mm.

The cranial termination of the EAS is of importance for the reproducibility of slice location, and several factors may impact on the identification of this structure. Commonly, the ventral and dorsal aspects of the EAS show "rotational asymmetry," that is, on average the EAS is slightly longer ven-

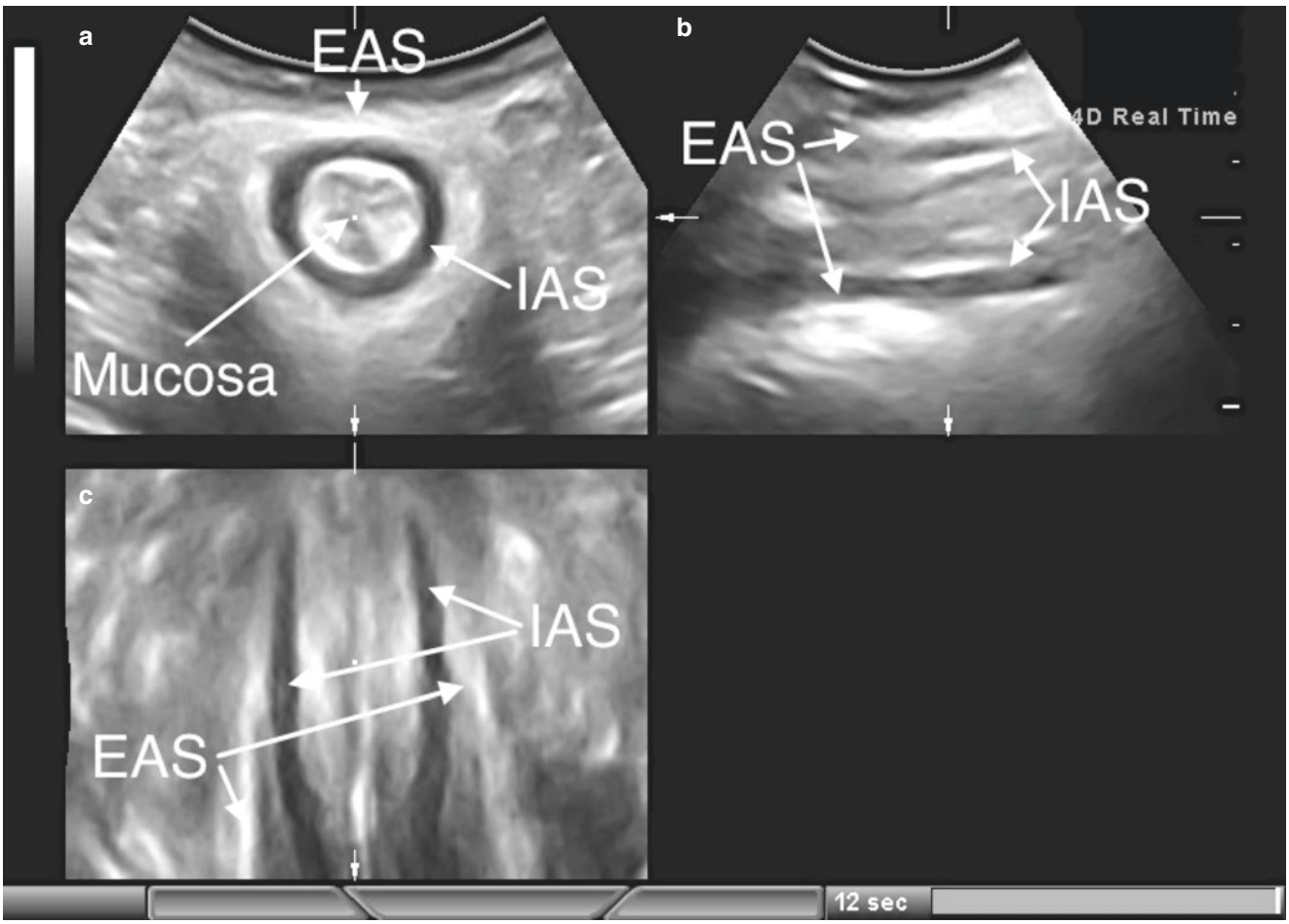

Fig. 6.15 Imaging of the anal sphincters in cross-sectional planes. The **a** plane shows the typical donut appearance of the external anal sphincter (EAS, hyperechogenic) and the internal anal sphincter (IAS, hypoechoic) in the coronal plane. The standard midsagittal orientation is given in the **b** plane, providing proof that the entire EAS is included in the volume. An oblique axial view is represented in the **c** plane and demonstrates that the anal canal is properly centered in the volume, i.e., seen as vertical in **c**. Reproduced with permission from [74]

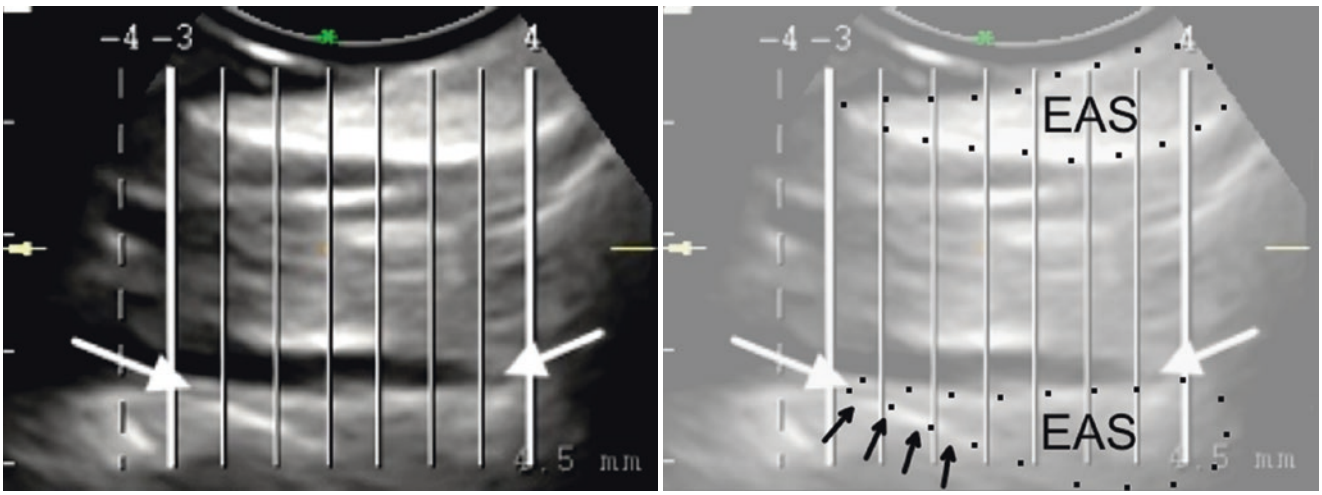

Fig. 6.16 A crucial step in translabial 4D sphincter imaging is the identification of the cranial limit of the external anal sphincter (EAS). This has to be obtained dorsally, at least in parous women, as the ventral aspect of the EAS may have been altered by birth trauma. The midsagittal plane (usually given in the plane of an orthogonal representation as in Figure 6.16) allows the identification of the fascial plane between EAS and levator ani (arrows)

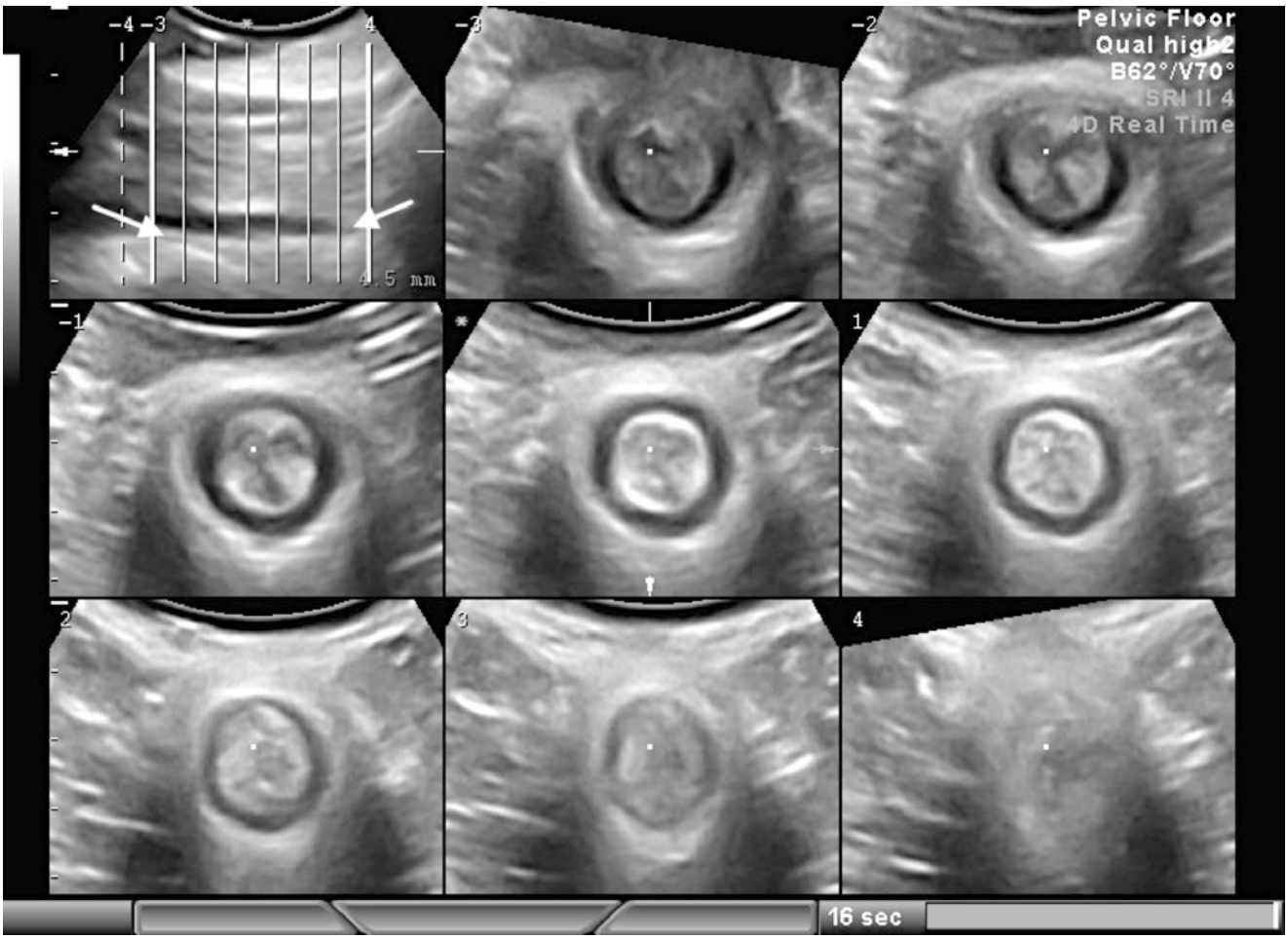

Fig. 6.17 Tomographic imaging of normal external and internal anal sphincters. The reference plane at the top left shows the midsagittal plane. Vertical lines indicate the location of eight coronal slices given in this figure. The most cranial slice (center top) is located above the external anal sphincter (EAS) (left thick line in the reference image); the most caudad (bottom right) is placed below the internal anal sphincter (right thick line) in the reference image. As a result, the entire EAS should be covered in this tomographic representation. From [32], with permission

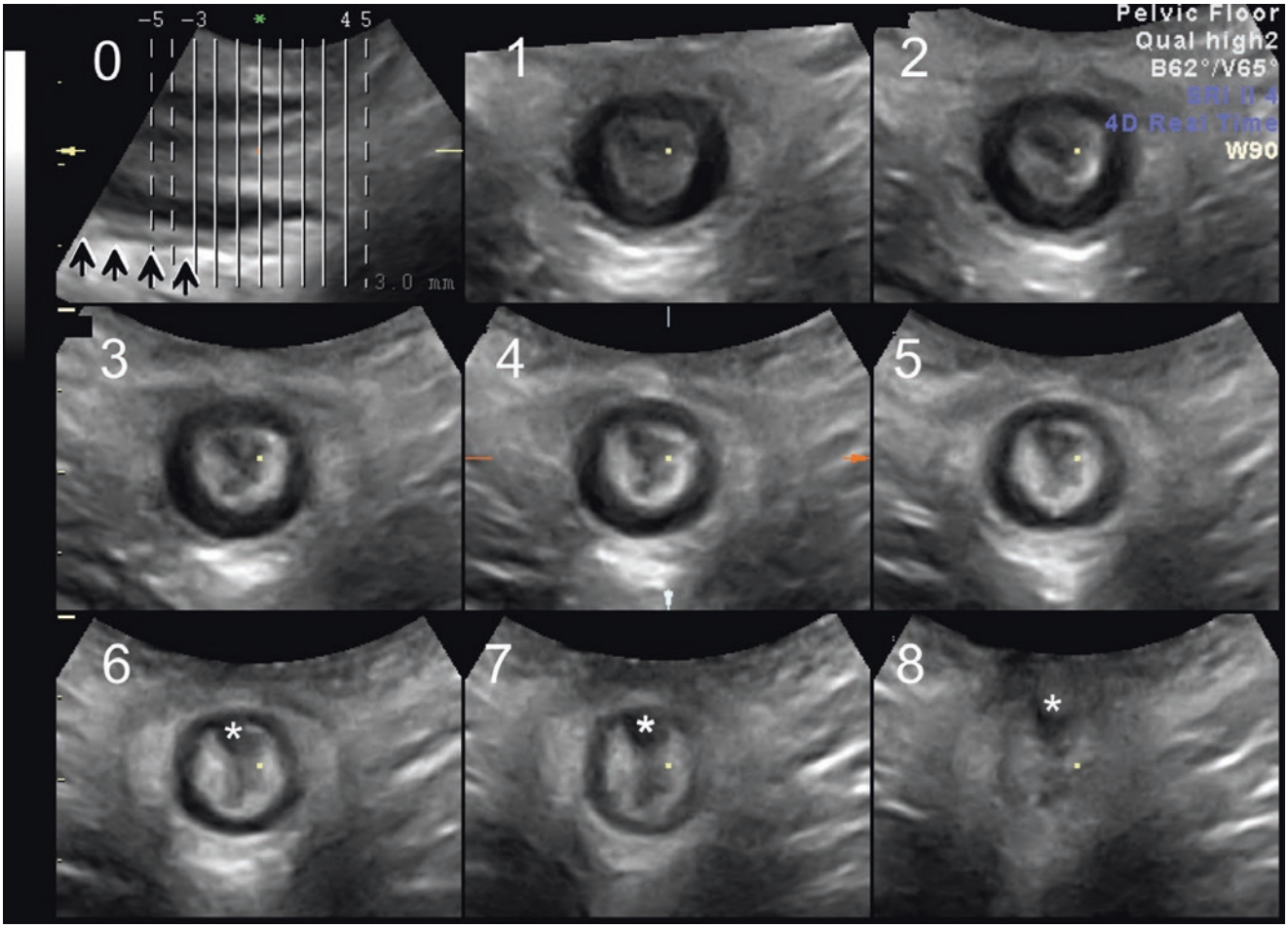

Fig. 6.18 Occasionally, a prominent LMA (longitudinal muscle of the anus, indicated by arrows) may interfere with locating the cranial margin of the external anal sphincter (EAS), as evident in the midsagittal reference plane (slice 0) given on the top left of this tomographic representation of the EAS. In such cases, the presumed "drop" shape of the EAS allows an estimation of its cranial limit, as given here. A small incidental hemorrhoid in slices 6–8 is indicated by (∗)

trally than dorsally, but the opposite may also occur. Such asymmetry however does not seem to affect diagnostic performance [33].

Occasionally, it is possible to distinguish separate components of the EAS, with the most distal component often being more echogenic than the more proximal component of the muscle. This can lead to ambiguity in the identification of the cranial EAS margin, since two fascial planes rather than one may be identified. In this situation one needs to use the more proximal of the two planes. Another source of inter-individual variation is the longitudinal muscle of the anus (LMA) which can be so thick as to resemble a cranial continuation of the EAS (Fig. 6.18). Sometimes the cranial termination of the EAS has to be extrapolated assuming a teardrop-shaped EAS. In practice, fortunately, these variations in anatomical appearance are of minor importance and unlikely to interfere with the diagnosis of sphincter trauma. Finally, it has to be mentioned that hemorrhoids can adversely affect imaging of the caudal aspects of the internal anal sphincter.

6.7 The Levator Ani Muscle

6.7.1 2D Imaging

The puborectalis muscle can be seen on 2D translabial ultrasound in a parasagittal plane, with the transducer tilted from dorsomedially to ventrolaterally as in Fig. 6.19 [34]. The fibers of the puborectalis muscle may be followed from the os pubis to the anal canal; more cranial aspects of the levator usually show a different fiber direction.

6.7.2 Axial Plane

Except when using obsolete side-firing vaginal transducers, access to the axial plane requires 3D/4D transducers, and this is the main reason why 4D imaging using abdominal volume probes has become such an asset to pelvic floor medicine over the last 10 years. Noninvasive, easy access to the

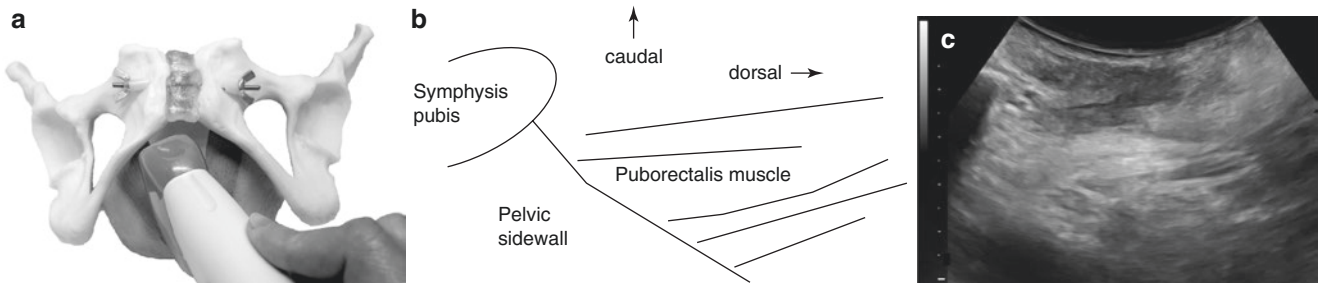

Fig. 6.19 Transducer orientation for imaging of the puborectalis muscle by translabial 2D ultrasound (left image), the resulting parasagittal view in a schematic drawing (center), and a normal muscle insertion on ultrasound, with the hyperechogenic muscle fibers clearly visible (right). Adapted from [34], with permission

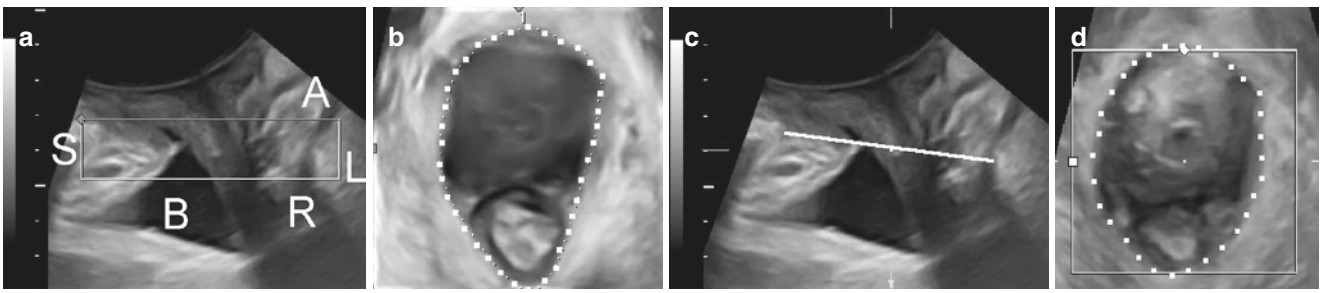

Fig. 6.20 Measuring hiatal dimensions as shown in a rendered volume (**a**, **b**) and in an oblique single axial plane (**c**, **d**). The region of interest (ROI) box in (**a**) (approx. 1.8 cm deep) is located between the symphysis pubis and the levator ani posterior to the anorectal angle. Image (**b**) represents a semitransparent view of all pixels in the ROI box on the left. The determination of hiatal dimensions using a single oblique axial plane is shown in (**c**) and (**d**). The midsagittal plane on the left (**c**) demonstrates a line indicating the minimal sagittal diameter of the hiatus, i.e., the location of the oblique axial plane shown in (**d**). The dotted line in (**b**) and (**d**) represents hiatal area measurements (21.77 cm2 in (**b**), 23.05 cm2 in (**d**)). *A* anal canal, *B* bladder, *L* levator ani, *R* rectum, *S* symphysis pubis. From [36], with permission

axial plane has led to this method largely replacing MRI for imaging of levator trauma, especially in the form of tomographic imaging. In addition, the levator hiatus, the largest potential hernial portal in the human body, can be imaged either as a single plane [35] or with the help of a "rendered volume" [36], i.e., a semitransparent representation of all volume pixels in a given space, a technology that was originally developed for fetal imaging (see Fig. 6.20). Both methods are equally valid and repeatable and allow quantification of the "levator hiatus," through which all forms of uterovaginal and anorectal prolapse can be seen to herniate out of the abdominal space.

Due to the requirements of childbirth, the hiatus is much larger in women than in men and constitutes a structural and functional compromise. The levator ani may be congenitally overdistensible [35] and vary between individuals and also between ethnic groups [35, 37], but "ballooning" [38] is clearly more likely in vaginally parous women due to the fact that childbirth enlarges hiatal dimensions [39]. Hiatal area is strongly associated with pelvic organ descent [41] and moderately with prolapse recurrence after pelvic reconstructive surgery [16, 40, 41], which makes it potentially useful in the investigation of women with pelvic floor disorders (see Chap. 48).

6.7.3 Multislice Imaging

Contrary to tomographic imaging with computed tomography (CT) and MRI, volume ultrasound produces not just a series of predetermined slices but rather a volume of information that allows us to alter slice orientation arbitrarily, after completion of an examination that takes only a few minutes. This has already been mentioned in the context of sphincter imaging, and it is equally useful in the assessment of the levator ani, the second major muscular structure to suffer permanent, clinically relevant damage in childbirth.

The primary component of the levator ani complex, both in childbirth and for pelvic organ support, is the puborectalis muscle, a V-shaped structure that inserts on the inferior pubic ramus and the body of the os pubis bilaterally, coursing around the anorectal junction posteriorly where it defines the anorectal angle. Dorsally the anococcygeal raphe anchors it to the coccyx, which explains the commonly used alternative anatomical term, pubococcygeus [42]. Figure 6.21 shows a comparison of graphic representation, dissection, and sonographic representation of the intact puborectalis muscle.

As opposed to the anal canal, we are unable to identify the cranial termination of the puborectalis muscle since it is in continuity with iliococcygeus and coccygeus muscles.

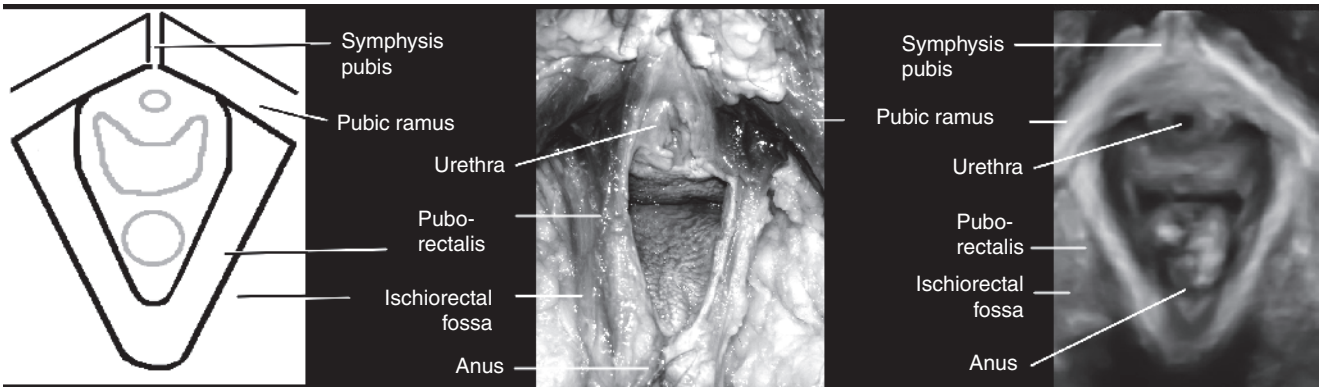

Fig. 6.21 Representation of the puborectalis muscle in a drawing (left), on cadaver dissection (middle), and in a rendered volume, axial plane (right)

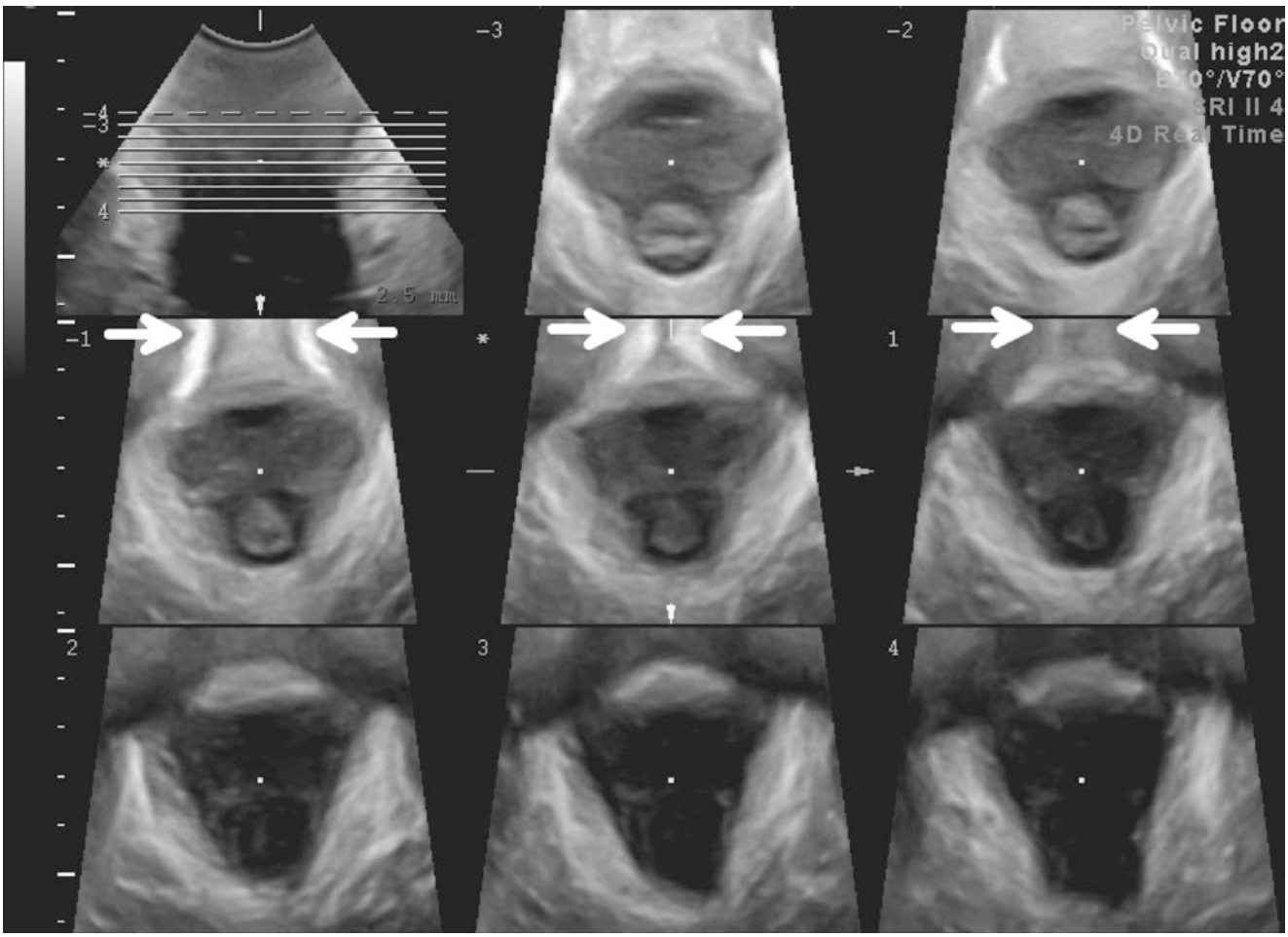

Fig. 6.22 Tomographic imaging of the puborectalis muscle in a nulliparous patient. The interstice interval is standardized to 2.5 mm. The central slice should show the most inferior aspect of the symphyseal gap, with the pubic rami appearing hyperechoic. The left central slice 2.5 mm caudad shows the pubic rami further apart. In the right central slice, the pubic rami are usually invisible due to acoustic shadowing. The arrows indicate the location of the pubic rami/the os pubis in the three central slices

Hence, we use the symphysis pubis as a reference structure, with the central slice placed approximately at the plane of minimal hiatal dimensions showing the symphysis pubis closing (Fig. 6.22). On tomographic representation, a 2.5 mm interslice interval allows coverage of the entire muscle [43]. While imaging on pelvic floor muscle contraction results in clearer images, assessment at rest may be equally valid [44, 45]. Using the minimum criterion of three central positive slices for the diagnosis of avulsion (see Chap. 48) [46], a false-positive diagnosis of avulsion seems unlikely [47]. In

Fig. 6.23 Measurement of the levator-urethra gap (LUG) between the center of the urethra and the insertion of the puborectalis can be helpful in difficult cases. The limits of normal for this measurement have been defined as 25 mm in Caucasians and 23.6 mm in East Asians

difficult cases, measurement of the "levator-urethra gap" or LUG (Fig. 6.23) is useful [48–50]. An equivalent measurement, the levator-symphysis gap or LSG, has been described on MRI [51]. Cutoffs of 25 mm in Caucasians [48] and 23.6 mm in East Asians [49] have been defined as limits of normality.

Function of the levator muscle can be ascertained by measuring muscle thickening and shortening on contraction, but indirect measures such as bladder neck lift or a reduction in hiatal dimensions are more practicable (see Fig. 6.24) and associated with other parameters of pelvic floor function [52, 53]. However, excellent pelvic floor functionality may not be evident in high-displacement measurements due to high resting tone and low tissue elasticity; sonographic measures of pelvic floor function may therefore not be superior to other measures of "strength" such as digital palpation or perineometry.

6.8 Static Versus Dynamic "Normality"

In clinical medicine, we commonly describe "static" normality which is quite often all there is to see and assess. An ovary looks "normal" or "not" – it has no "dynamic" normality. The pelvic floor is very different in this regard however. Most pelvic floor dysfunction is due to abnormalities of dynamic anatomy or function. Female pelvic organ prolapse, obstructed defecation, and stress urinary incontinence are disorders of functional anatomy—problems usually only become apparent once support structures are put under strain.

The degree of strain is essential when it comes to measuring organ descent. Assessment of organ descent during a Valsalva maneuver performed in the supine position after bladder emptying [54] shows good test characteristics even if Valsalva pressure is not controlled [55], provided it is performed over a time period of at least 6 s [56] and provided levator co-activation is avoided [57]. Figure 6.25 demonstrates the importance of an optimal Valsalva maneuver. Assessment in the standing position will result in lower organ location, but test characteristics are not improved compared to the supine position [58].

Normality of a quantitative measure such as organ descent can be defined in at least two ways: mathematically as the mean plus/minus two standard deviations and against symptoms arising from abnormal anatomy, i.e., symptoms of stress urinary incontinence in the case of urethral mobility and bladder neck configuration and symptoms of prolapse in the case of pelvic organ mobility. The mathematical approach to defining normality requires assessment of nulliparae, since pregnancy and childbirth are clearly the main environmental confounder. The second approach is appropriate in a population in which symptoms are common, e.g., in women who seek assessment or treatment for manifestations of pelvic floor dysfunction.

6.9 Urethral Mobility and Bladder Neck Configuration

Excessive *bladder neck descent* or "hypermobility" has been commonly thought to be responsible for stress urinary incontinence (SUI) and urodynamic stress incontinence (USI), but "hypermobility" of the bladder neck is usually not defined numerically. Bladder neck descent as shown in Fig. 6.26 varies greatly in young, healthy, asymptomatic women [59] and is likely to be genetically determined [60]. It varies between ethnic groups [61–63] and is associated with stress urinary incontinence [64, 65]. This association between stress continence and bladder neck mobility is consistent with the concept of force or pressure transmission through "pubourethral ligaments" (see above): the more mobile the urethra, the greater the likelihood of poor function of these ligaments, and the poorer may be pressure transmission. This concept is supported by the observation that mobility at the locus of urethral tethering by pubourethral structures, the mid-urethra, is more strongly associated with continence than bladder neck mobility [19].

Recent work suggests a cutoff of 25 mm for the definition of "bladder neck hypermobility" [66]. However, its associa-

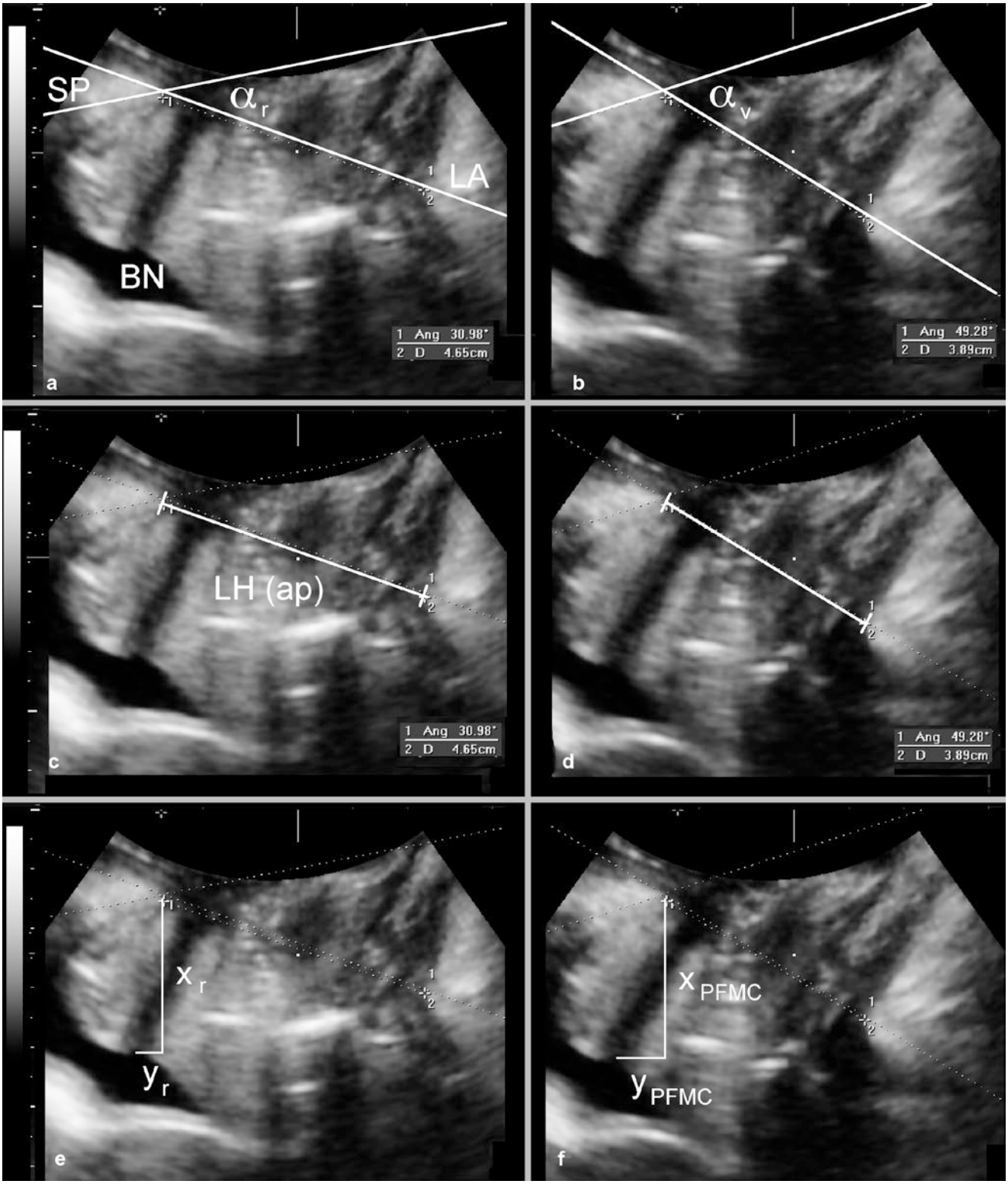

Fig. 6.24 Three methods of determining the effect of a pelvic floor muscle contraction (PFMC) in the midsagittal plane, using 2D translabial ultrasound. The left-hand images in each pair (**a**, **c**, **e**) represent the resting state; the right-hand images show findings on PFMC. The top pair illustrates measurement of the levator plate angle (angle between symphyseal axis and levator hiatus in the midsagittal plane), the middle pair shows reduction of the anteroposterior diameter of the levator hiatus (LH (ap)), and the bottom pair illustrates bladder neck (BN) displacement on PFMC, analogous to the way BN descent is measured on Valsalva. *LA* levator ani, *SP* symphysis pubis. From [53], with permission

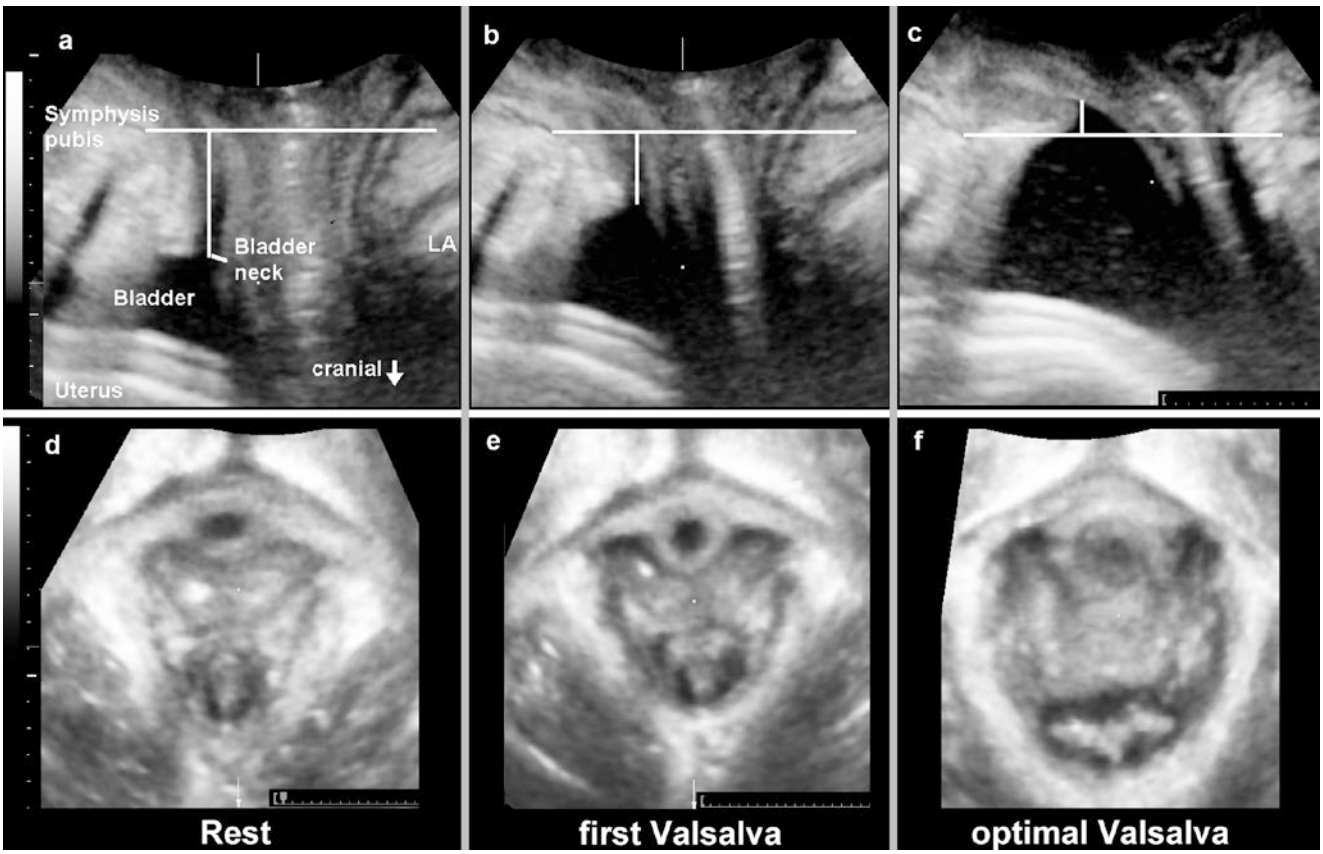

Fig. 6.25 Levator co-activation as a confounder of Valsalva effort. The top row of images shows the midsagittal, and the bottom row the axial plane. **a** and **d** demonstrate findings at rest, **b** and **e** a suboptimal Valsalva confounded by pelvic floor muscle (PFM) activation, and **c** and **f** a full, appropriate Valsalva. It is evident that, while there is some bladder neck descent on Valsalva in (**b**), the levator hiatus in e is in fact smaller than in (**d**), indicating a confounding PFM contraction. *LA* levator ani. Adapted from [57] with permission

tion with stress urinary incontinence is barely strong enough to use the "symptoms" approach to determining normality, with an area under the curve of 0.61 on ROC statistics, and the mathematical approach (mean + 2SD) in young Caucasian nulliparae would yield 35 mm [59].

The association between *proximal urethral rotation* and *retrovesical angle* on the one hand and stress continence on the other hand is even weaker, with AUCs below 0.6 [66]. However, an "open" retrovesical angle (RVA) of 140° or higher and proximal urethral rotation of >45° have been identified as the "anatomical correlate" of stress urinary incontinence since the 1960s [67, 68]. This has been confirmed on translabial ultrasound [66]; hence, it seems reasonable to define an RVA of <140° and proximal urethral rotation of up to 45° as normal.

6.10 Pelvic Organ Descent

Organ descent is measured after bladder emptying, supine, and on maximal Valsalva of at least 6 s duration, controlling for levator co-activation [56]. The best of three maneuvers is chosen for numerical evaluation. Figure 6.27 shows the measurement of organ descent against a horizontal line placed through the inferior margin of the symphysis pubis. There is limited information on the "normality" of pelvic organ descent in young nulliparous women. In the previously mentioned study in 116 nulligravid 18–24-year-old Caucasians asymptomatic of prolapse, the mean plus two SD yielded potential cutoffs of 6 mm below the symphysis pubis for bladder descent, of 5 mm above for uterine descent, and of 24 mm below the symphysis for descent of the rectal ampulla [69]. These figures are rather close to values obtained by using the "symptoms" approach, i.e., by utilizing ROC curve statistics in large symptomatic cohorts. This latter approach yields cutoffs of 10 mm below the SP for bladder descent, of 15 mm above the SP for uterine descent, and of 15 mm below the SP for descent of the rectal ampulla [69].

Recent work using clinical prolapse assessment [70] has confirmed that "normality" of pelvic organ mobility needs to be redefined, since descent of the uterus to a given level is much more likely to cause symptoms of prolapse than descent of the anterior or posterior compartments. Current clinical usage of the ICS

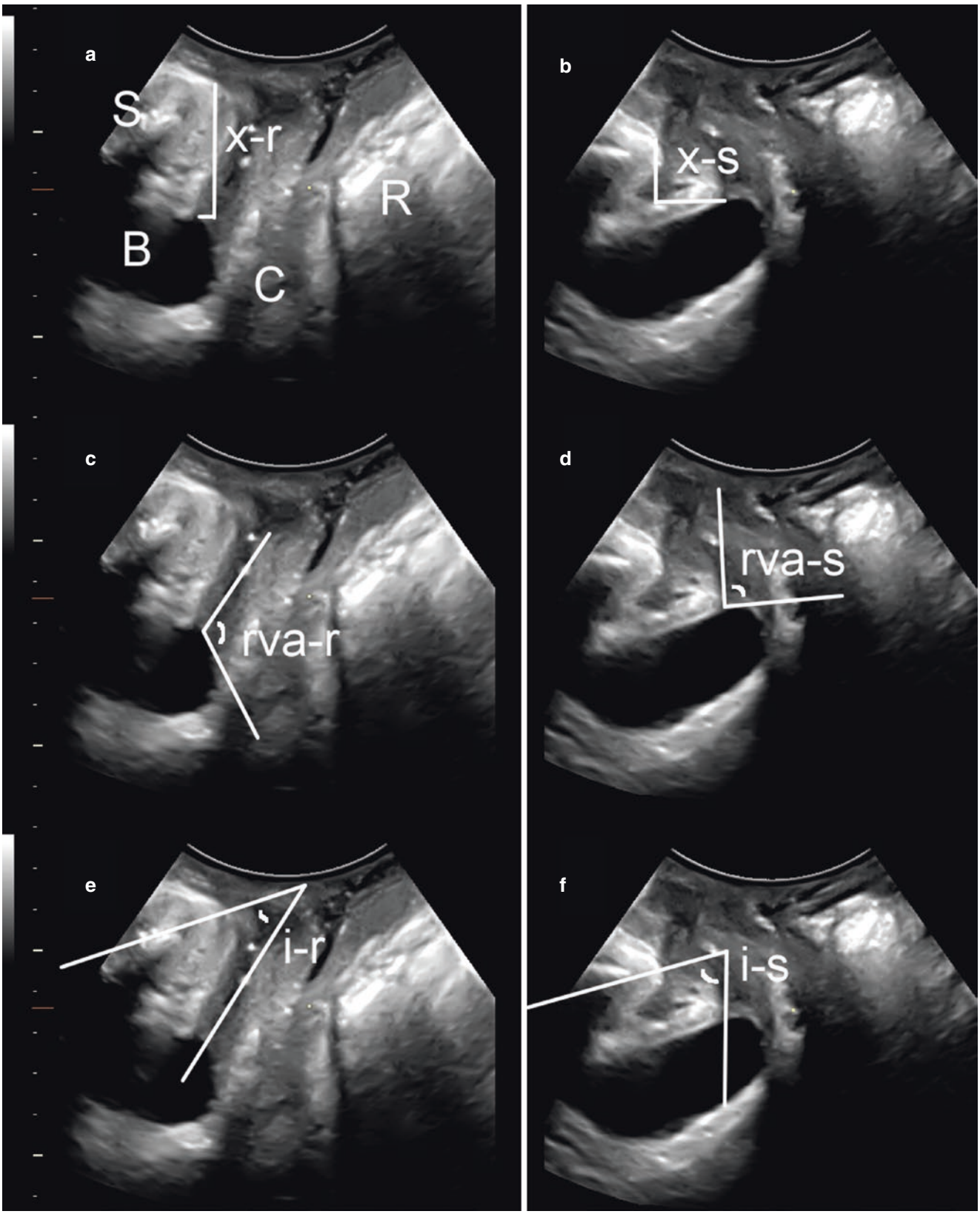

Fig. 6.26 Normal mobility of the bladder and urethra demonstrated on Valsalva. The left image in all three panels is obtained at rest, the right on maximal Valsalva. "x" and "y" illustrate horizontal and vertical coordinates used to determine bladder neck mobility in **a** and **b**. "Bladder neck descent" is the vertical component of this movement, i.e., x-r (rest) minus x-s (Valsalva) or, as in this case, 29 mm − 14 mm = 15 mm. In panel **c** and **d**, "rva" is the retrovesical angle given at rest (rva-r, 120°) and on Valsalva (rva-s, 85°). In panel **e** and **f**, urethral rotation is determined by comparing the angle between the central symphyseal axis and the proximal urethra (i-s [60°] minus i-r [35°] = 25°). *B* bladder, *C* cervix, *R* rectal ampulla, *S* symphysis pubis

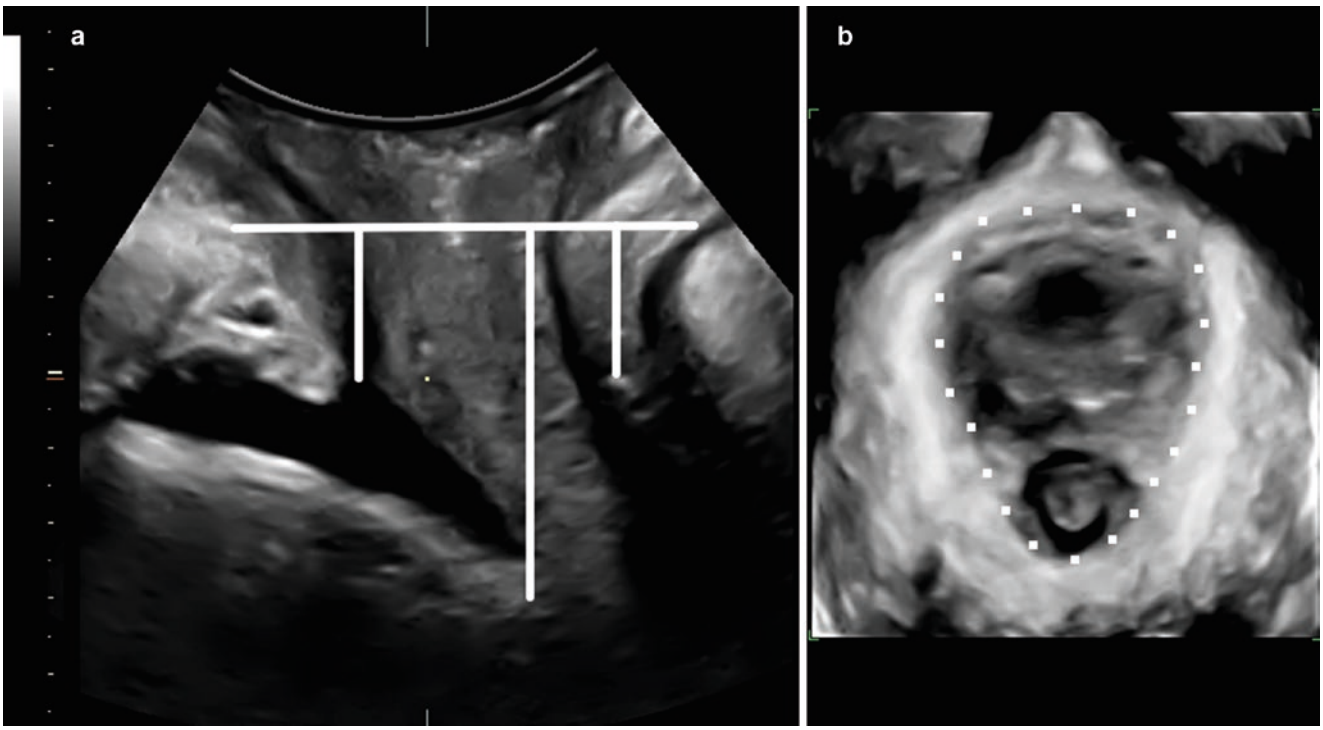

Fig. 6.27 Quantification of organ decent and hiatal area in patient with normal organ support, midsagittal plane. Organ descent is measured against a horizontal line placed through the inferoposterior margin of the symphysis pubis (**a**). Panel **b** shows measurement of the levator hiatus

POP-Q assessment system [71] may result in abnormal uterine descent being rated as normal, while a "second-degree cystocele" may be diagnosed in a woman with normal bladder mobility.

6.11 Hiatal Dimensions

The same approach, i.e., the "mathematical" and the "symptoms" approach, may be used to determine normal values for hiatal distensibility. Maximal hiatal distension on Valsalva in the axial plane is known to be strongly associated with POP and POP symptoms [35, 38], and this is also evident on clinical examination using measurements of the genital hiatus and perineal body [72, 73]. Conveniently, both "mathematical" and "symptoms" approaches yield virtually identical cutoffs when measured in volume data obtained on maximal Valsalva in the supine position: 25.79 cm^2 in 18–24-year-old Caucasian nulliparae [35] and 25 cm^2 in symptomatic older women [38]. Hence, it is suggested that 25 cm^2 be used as the limit of normality for hiatal distension on Valsalva.

6.12 Conclusions

In this chapter I have tried to cover imaging of the normal pelvic floor by pelvic floor ultrasound, with "normality" defined not just in the sense of static anatomy but also as "dynamic normality" so that pelvic organ mobility and hiatal dimensions under conditions of elevated intra-abdominal pressure can be classified as normal or abnormal. Chapter 48 will deal with abnormality, both static and dynamic.

Take-Home Messages

- Translabial pelvic floor ultrasound is the best-documented and most convenient imaging method currently in use in pelvic floor medicine.
- Simple 2D systems, available since the 1980s, provide information on organ descent, residual urine, bladder neck configuration, and urethral anatomy and mobility.
- 3D/4D imaging via the translabial route allows axial plane imaging of the levator ani and anal sphincter.
- In combination with tomographic or multislice imaging, this enables quick, noninvasive assessment of both structures by standardized, validated methods.
- Online interactive teaching is available through the International Urogynecological Association (IUGA) at https://www.iuga.org/education/pfic/pfic-overview.

References

1. Dietz H. Ultrasound imaging of the pelvic floor: part 1: 2D aspects. Ultrasound Obstet Gynecol. 2004;23:80–92.
2. Dietz H, Cartmill J. Imaging in patients with obstructed defecation. Tech Coloproctol. 2013;17:473–4.
3. Dietz H. Ultrasound imaging of the pelvic floor. Part II: three-dimensional or volume imaging. Ultrasound Obstet Gynecol. 2004;23(6):615–25.
4. Dietz H. Quantification of major morphological abnormalities of the levator ani. Ultrasound Obstet Gynecol. 2007;29:329–34.
5. Guzman Rojas R, Shek KL, Langer SM, Dietz HP. Prevalence of anal sphincter injury in primiparous women. Ultrasound Obstet Gynecol. 2013;42(4):461–6.
6. Dietz HP, Pardey J, Murray HG. Maternal birth trauma should be a key performance indicator of maternity services. Int Urogynecol J. 2015;26:29–32.
7. Grischke EM, Dietz HP, Jeanty P, Schmidt W. A new study method: the perineal scan in obstetrics and gynecology. Ultraschall Med. 1986;7(4):154–61.
8. Olsen AL, et al. Epidemiology of surgically managed pelvic organ prolapse and urinary incontinence. Obstet Gynecol. 1997;89(4):501–6.
9. Smith F, Holman CD, Moorin RE, Tsokos N. Lifetime risk of undergoing surgery for pelvic organ prolapse. Obstet Gynecol. 2010;116:1096–100.
10. Svabik K, Shek K, Dietz H. How much does the levator hiatus have to stretch during childbirth? Br J Obstet Gynaecol. 2009;116:1657–62.
11. Dietz H, Lanzarone V. Levator trauma after vaginal delivery. Obstet Gynecol. 2005;106:707–12.
12. Shek K, Dietz H. Intrapartum risk factors of levator trauma. Br J Obstet Gynaecol. 2010;117:1485–92.
13. Dietz HP, Chantarasorn V, Shek KL. Levator avulsion is a risk factor for cystocele recurrence. Ultrasound Obstet Gynecol. 2010;36:76–80.
14. Model A, Shek KL, Dietz HP. Levator defects are associated with prolapse after pelvic floor surgery. Eur J Obstet Gynecol Reprod Biol. 2010;153:220–3.
15. Weemhoff M, Vergeldt TF, Notten K, Serroyen J, Kampschoer PH, Roumen FJ. Avulsion of puborectalis muscle and other risk factors for cystocele recurrence: a 2-year follow-up study. Int Urogynecol J. 2012;23(1):65–71.
16. Vergeldt T, Notten K, Weemhoff M, van Kuijk S, Mulder F, Beets-Tan R, et al. Levator hiatal area as a risk factor for cystocele recurrence after surgery: a prospective study. Br J Obstet Gynaecol. 2015;122(8):1130–7.
17. Dietz HP. Forceps: towards obsolescence or revival? Acta Obstet Gynecol Scand. 2015;94(4):347–51.
18. El Sayed R, Morsy MM, el-Mashed SM, Abedl-Azim MS. Anatomy of the urethral supporting ligaments defined by dissection, histology, and MRI of female cadavers and MRI of healthy nulliparous women. AJR. 2007;189:1145–57.
19. Pirpiris A, Shek KI, Dietz HP. Urethral mobility and urinary incontinence. Ultrasound Obstet Gynecol. 2010;36:507–11.
20. Khullar V. Ultrasonography. In: Cardozo L, Staskin D, editors. Textbook of female urology and urogynaecology. London: Isis Medical Media; 2001. p. 300–12.
21. Khullar V, Cardozo LD, Salvatore S, Hills S. Ultrasound: a noninvasive screening test for detrusor instability. Br J Obstet Gynaecol. 1996;103(9):904–8.
22. Lekskulchai O, Dietz H. Detrusor wall thickness as a test for detrusor overactivity in women. Ultrasound Obstet Gynecol. 2008;32:535–9.
23. Yang JM, Huang WC. Bladder wall thickness on ultrasound cystourethrography. J Ultrasound Med. 2003;22:777–82.
24. Nguyen JK, Hall CD, Taber E, Bhatia NN. Ultrasonographid diagnosis of paravaginal defects: a critical evaluation. Int Urogynecol J. 1999;10(S1):S52.
25. Dietz HP, Pang S, Korda A, Benness C. Paravaginal defects: a comparison of clinical examination and 2D/3D ultrasound imaging. Aust NZ J Obstet Gynaecol. 2005;45:187–90.
26. Garriga J, et al. Can we identify changes in fascial paravaginal supports after childbirth? Aust NZ J Obstet Gynaecol. 2015;55:70–5.
27. Chantarasorn V, Shek K, Dietz HP. Sonographic appearance of the perineal body and changes in mobility after childbirth. Int Urogynecol J. 2012;23(6):729–33.
28. Richardson AC. The anatomic defects in rectocele and enterocele. J Pelvic Surg. 1996;1:214–21.
29. Dietz HP. Can the rectovaginal septum be visualised on ultrasound? Ultrasound Obstet Gynecol. 2011;37(4):348–52.
30. Dietz HP, Clarke B. The prevalence of rectocele in young nulliparous women. Aust NZ J Obstet Gynaecol. 2005;45:391–4.
31. Young N, Atan I, Dietz HP. Obesity: how much does it matter for female pelvic organ prolapse? Int Urogynecol J. 2018;29(8):1129–34.
32. Dietz HP. Exo-anal imaging of the anal sphincters: a pictorial introduction. J Ultrasound Med. 2018;37:263–80.
33. Magpoc J, Kamisan Atan I, Dietz HP. Normal values of anal sphincter biometry by four-dimensional pelvic floor ultrasound. Int Urogynecol J. 2016;27(S1):S113–4.
34. Dietz HP, Shek KL. Levator defects can be detected by 2D translabial ultrasound. Int Urogynecol J. 2009;20:807–11.
35. Dietz H, Shek K, Clarke B. Biometry of the pubovisceral muscle and levator hiatus by three-dimensional pelvic floor ultrasound. Ultrasound Obstet Gynecol. 2005;25:580–5.
36. Dietz H, Wong V, Shek KL. A simplified method for determining hiatal biometry. Aust NZ J Obstet Gynaecol. 2011;51:540–3.
37. Cheung R, Shek KL, Chan SS, Chung TK, Dietz HP. Pelvic floor biometry and pelvic organ mobility in Asian and Caucasian nulliparae. Int Urogynecol J. 2013;24(S1):S53–5.
38. Dietz H, De Leon J, Shek K. Ballooning of the levator hiatus. Ultrasound Obstet Gynecol. 2008;31:676–80.
39. Kamisan Atan I, Gerges B, Shek KL, Dietz HP. The association between vaginal childbirth and hiatal dimensions: a retrospective observational study in a tertiary urogynaecological centre. BJOG. 2015;122(6):867–72.
40. Rodrigo N, Wong V, Shek KL, Martin A, Dietz HP. The use of 3-dimensional ultrasound of the pelvic floor to predict recurrence risk after pelvic reconstructive surgery. Aust NZ J Obstet Gynaecol. 2014;54(3):206–11.
41. Friedman T, Eslick G, Dietz HP. Risk factors for prolapse recurrence—systematic review and meta-analysis. Int Urogynecol J. 2018;29(1):13–21.
42. DeLancey JO. The anatomy of the pelvic floor. Curr Opin Obstet Gynecol. 1994;6(4):313–6.
43. Kashihara H, Shek K, Dietz H. Can we identify the limits of the puborectalis/ pubovisceralis muscle on tomographic translabial ultrasound? Ultrasound Obstet Gynecol. 2012;40(2):219–22.
44. van Delft K, Thankar R, Sultan AH, Kluivers KB. Does the prevalence of levator ani muscle avulsion differ when assessed using tomographic ultrasound imaging at rest vs on maximum pelvic floor muscle contraction? Ultrasound Obstet Gynecol. 2015;46(1):99–103.
45. Dietz H, Pattillo Garnham A, Guzmán Rojas R. Diagnosis of levator avulsion: is it necessary to perform TUI on pelvic floor muscle contraction? Ultrasound Obstet Gynecol. 2017;49(3):252–6.
46. Dietz H, Bernardo MJ, Kirby A, Shek KL. Minimal criteria for the diagnosis of avulsion of the puborectalis muscle by tomographic ultrasound. Int Urogynecol J. 2011;22(6):699–704.
47. Adisuroso T, Shek K, Dietz H. Tomographic imaging of the pelvic floor in nulliparous women: limits of normality. Ultrasound Obstet Gynecol. 2012;39(6):698–703.

48. Dietz H, Abbu A, Shek K. The levator urethral gap measurement: a more objective means of determining levator avulsion? Ultrasound Obstet Gynecol. 2008;32:941–5.
49. Zhuang R, Song YF, Chen ZQ, et al. Levator avulsion using a tomographic ultrasound and magnetic resonance-based model. Am J Obstet Gynecol. 2011;205:232.e1–8.
50. Dietz H, Pattillo Garnham A, Guzman Rojas R. Is the levator-urethra gap helpful for the diagnosis of avulsion? Int Urogynecol J. 2016;27(6):909–13.
51. Singh K, Jakab M, Reid WMN, Berger LA, Hoyte L. Three-dimensional magnetic resonance imaging assessment of levator ani morphologic features in different grades of prolapse. Am J Obstet Gynecol. 2003;188(4):910–5.
52. Dietz HP, Jarvis SK, Vancaillie TG. The assessment of levator muscle strength: a validation of three ultrasound techniques. Int Urogynecol J. 2002;13(3):156–9.
53. Dietz HP. Pelvic floor ultrasound in incontinence: what's in it for the surgeon? Int Urogynecol J. 2011;22(9):1085–97.
54. Dietz HP, Haylen BT, Broome J. Ultrasound in the quantification of female pelvic organ prolapse. Ultrasound Obstet Gynecol. 2001;18(5):511–4.
55. Mulder F, Shek K, Dietz H. The pressure factor in the assessment of pelvic organ mobility. Aust NZ J Obstet Gynaecol. 2012;52:282–5.
56. Orejuela F, Shek K, Dietz H. The time factor in the assessment of prolapse and levator ballooning. Int Urogynecol J. 2012;23:175–8.
57. Oerno A, Dietz H. Levator co-activation is a significant confounder of pelvic organ descent on Valsalva maneuver. Ultrasound Obstet Gynecol. 2007;30:346–50.
58. Rodríguez-Mias NL, Subramaniam N, Friedman T, et al. Prolapse assessment supine and standing: do we need different cutoffs for "significant prolapse"? Int Urogynecol J. 2018;29(5):685–9.
59. Dietz HP, Eldridge A, Grace M, Clarke B. Pelvic organ descent in young nulligravid women. Am J Obstet Gynecol. 2004;191(1):95–9.
60. Dietz H, Hansell NK, Grace ME, Eldridge AM, Clarke B, Martin NG. Bladder neck mobility is a heritable trait. Br J Obstet Gynaecol. 2005;112:334–9.
61. Dietz HP. Do Asian women have less pelvic organ mobility than Caucasians? Int Urogynecol J. 2003;14(4):250–3.
62. Shek KL, Krause H, Wong V, Goh J, Dietz HP. Is pelvic organ support different between young nulliparous Africans and Caucasians? Ultrasound Obstet Gynecol. 2016;47(6):774–8.
63. Abdool Z, Dietz HP, Lindeque G. Interethnic variation in pelvic floor morphology in women with symptomatic pelvic organ prolapse. Int Urogynecol J. 2018;29(5):745–50.
64. Dietz HP, Clarke B. The urethral pressure profile and ultrasound imaging of the lower urinary tract. Int Urogynecol J. 2001;12(1):38–41.
65. Dietz H, Nazemian K, Shek KL, Martin A. Can urodynamic stress incontinence be diagnosed by ultrasound? Int Urogynecol J. 2013;24(8):1399–403.
66. Naranjo-Ortiz C, Shek KL, Dietz HP. What is normal bladder neck anatomy? Int Urogynecol J. 2016;27(6):945–50.
67. Green TH Jr. The problem of urinary stress incontinence in the female: an appraisal of its current status. Obstet Gynecol Surv. 1968;23(7):603–34.
68. Green TH Jr. Static cystourethrograms in stress urinary incontinence. Am J Obstet Gynaecol. 1978;132(2):228–32.
69. Shek KL, Dietz HP. Assessment of pelvic organ prolapse: a review. Ultrasound Obstet Gynecol. 2016;48:681–92.
70. Dietz H, Mann K. What is clinically relevant prolapse? An attempt at defining cutoffs for the clinical assessment of pelvic organ descent. Int Urogynecol J. 2014;25:451–5.
71. Bump RC, Mattiasson A, Bo K, et al. The standardization of terminology of female pelvic organ prolapse and pelvic floor dysfunction. Am J Obstet Gynecol. 1996;175(1):10–7.
72. Khunda A, Shek K, Dietz H. Can ballooning of the levator hiatus be determined clinically? Am J Obstet Gynecol. 2012;206(3):246.e1–4.
73. Gerges B, Kamisan Atan I, Shek KL, Dietz HP. How to determine "ballooning" of the levator hiatus on clinical examination: a retrospective observational study. Int Urogynecol J. 2013;24:1933–7.
74. Dietz HP. Pelvic floor ultrasound. In: Fleischer AC, Toy E, Manning F, et al., editors. Sonography in obstetrics and gynecology: principles and practice. 8th ed. New York, NY: McGrawHill; 2017.
75. Dietz HP. Pelvic floor assessment: a review. Fetal Matern Med Rev. 2009;20:49–66.